Inhibition of vascular endothelial growth factor receptor under hypoxia causes severe, human-like pulmonary arterial hypertension in mice: Potential roles of interleukin-6 and…

TRAN VAN HUNG

(Degree)
博士（医学）

(Date of Degree)
2014-03-25

(Date of Publication)
2015-03-01

(Resource Type)
doctoral thesis

(Report Number)
甲第6050号

(URL)
https://hdl.handle.net/20.500.14094/D1006050

Inhibition of vascular endothelial growth factor receptor under hypoxia causes severe, human-like pulmonary arterial hypertension in mice: Potential roles of interleukin-6 and endothelin

低酸素環境下における血管内皮細胞増殖因子受容体阻害による重症ヒト肺動脈性肺高血圧症に類似した病態モデルマウスの作製：インターロイキン６とエンドセリンの役割についての検討

Hung Tran Van, Noriaki Emoto, Nicolas Vignon-Zellweger, Kazuhiko Nakayama, Keiko Yagi, Yoko Suzuki, Ken-ichi Hirata

神戸大学大学院医学研究科内科系講座
循環器内科学分野
（指導教員：平田 健一 教授）

Tran Van Hung

Key words: Interleukin-6, Endothelin-1, Pulmonary arterial hypertension, Macrophage

Inhibition of vascular endothelial growth factor receptor under hypoxia causes severe, human-like pulmonary arterial hypertension in mice: Potential roles of interleukin-6 and endothelin

Hung Tran Van [a], Noriaki Emoto[a,b], Nicolas Vignon-Zellweger[b], Kazuhiko Nakayama [a, b], Keiko Yagi[b], Yoko Suzuki [b], Ken-ichi Hirata [a]

[a]Division of Cardiovascular Medicine, Department of Internal Medicine, Kobe University Graduate School of Medicie, Kobe, Japan

[b]Department of Clinical Pharmacy, Kobe Pharmaceutical University, Kobe, Japan

Running Head: IL-6 and the endothelin system in pulmonary arterial hypertension

Corresponding Authors:
Noriaki Emoto
Division of Cardiovascular Medicine
Department of Internal Medicine
Kobe University Graduate School of Medicine
7-5-1, Kusunoki, Chuo
Kobe, 650-0017 Japan
Tel.: +81-78-382-5846; Fax: +81-78-382-5859
E-mail: emoto@med.kobe-u.ac.jp

Keywords: Interleukin-6; Endothelin-1; Pulmonary arterial hypertension; Macrophage

ABSTRACT

Aims: Severe pulmonary arterial hypertension (PAH) is an incurable disease whose exact mechanisms remain unknown. However, growing evidence highlights the role of inflammation and endothelin (ET) signaling. The lack of reliable models makes it difficult to investigate the pathophysiology of this disease. Our aim was therefore to develop a mouse model of severe PAH closely mimicking human condition to explore the role of Interleukin-6 (IL-6), and ET signaling in advanced PAH progression.

Main methods: Young male SV129 mice received vascular endothelial growth factor receptor (VEGF-R) inhibitor (SU5416) (20 mg/kg) three times a week and were exposed to hypoxia (10% O_2) for three weeks. Molecular analysis and histological assessment were examined using real-time PCR, Western blot and immunostaining, respectively.

Key findings: The developed murine model presented important characteristics of severe PAH in human: concentric neointimal wall thickening, plexogenic lesions, recruitment of macrophages, and distal arteriolar wall muscularization. We detected an increase of IL-6 production and a stronger macrophage recruitment in adventitia of remodeled arterioles developing plexogenic lesions. Moreover, ET-1 and ET receptor A were up-regulated in lung lysates and media of remodeled arterioles. Recombinant IL-6 (50ng/ml) stimulated the proliferation and regulated endothelial cells in increasing ET-1 and decreasing ET receptor B.

Significance: These data describe a murine model, which displays the most important features of human severe PAH. We assume that inflammation, particularly IL-6 regulating ET signaling, plays a crucial role in forming plexogenic lesions. This model is thus reliable and might be used for a better understanding of severe PAH progression and treatment.

INTRODUCTION

Pulmonary artery hypertension (PAH) is featured by aberrant inflammation, vasoconstriction and remodeling in small pulmonary arteries (PA) (Voelkel and Tuder, 1997). PA high pressure induces right ventricular (RV) hypertrophy, failure and ultimately death (Humbert et al., 2004; Tuder et al., 2001b). Severe PAH is characterized by hyperproliferation of PA smooth muscle cells (SMCs) and endothelial cells (ECs), creating medial and concentric neointimal thickening, and arteriolar lumens' obliteration, leading to plexogenic lesions (Pietra et al., 2004; Tuder et al., 1994). Current therapies including prostacyclins, endothelin receptor antagonists (ERA), and phosphodiesterase-5 inhibitors, focus on pulmonary arterial endothelial cell (PAEC) dysfunctions but not their hyperproliferation (Archer et al., 2010), hence, the annual mortality is still up to 15% (Thenappan et al., 2007). This relative inefficacy highlights a strong demand in animal modeling with recapitulative pathophysiological changes of severe PAH.

Although the prognosis of patients with inflammation-associated PAH (i.e. connective tissue disease- (CTD-) associated PAH, particularly systemic sclerosis- (SSc-) associated PAH) improved recently, it is still worse than that of idiopathic PAH (iPAH) (Condliffe et al., 2009; Fisher et al., 2006; Girgis et al., 2005; Kawut et al., 2003). While inflammatory disturbances are described in both iPAH and SSc-PAH, these aberrancies are more severe in SSc-PAH, which explains the clinical and outcome discrepancies between the two syndromes (Fisher et al., 2006; Hassoun et al., 2009; Kawut et al., 2003). This suggests an inappropriate control of inflammation in the treatment of severe PAH.

Interleukin-6 (IL-6) concentration in patient plasma and lung tissues correlates with the severity and prognosis of the disease (Soon et al., 2010). IL-6 is elevated in most forms of PAH, especially CTD-PAH (Hassoun et al., 2009; Humbert et al., 1995; Itoh et al., 2006; Lesprit et al.,

1998). Subcutaneous injection of recombinant IL-6 (rIL-6) in rats (Miyata et al., 2001) and mice (Golembeski et al., 2005) induced PAH determined by medial thickening of small PA, Fulton index and right ventricular systolic pressure (RVSP), while IL-6 transgenic (IL-6 Tg+) mice spontaneously developed PAH with neointimal hyperplasia (Steiner et al., 2009). Moreover, IL-6 knockout mice were resistant to increase RVSP under hypoxia (Savale et al., 2007). It is suggestible about the role of IL-6 in stimulating the proliferation of ECs and SMCs (Steiner et al., 2009; Yao et al., 2006, 2007) leading to severe PAH. However, the source and mechanism of IL-6 at the injured sites are questionable. In experimental PAH, increased inflammatory cells around and in remodeled lesions are accompanied with elevated cytokines/chemokines including IL-6 and monocyte chemotactic protein-1 (MCP-1). In those models, PAH can be reversed or prevented by an anti-inflammation treatment (Burke et al., 2009; Mizuno et al., 2012; Price et al., 2011). In PAH patients, macrophages accumulate around the plexogenic lesions (Tuder et al., 1994). We therefore investigated whether IL-6 produced by the recruited macrophages at the injured sites promoted the development of arteriopathy and consequent severe PAH.

Endothelin-1 (ET-1) is a potent endogenous vasoconstrictor produced by ECs, acting via two receptors, endothelin receptor A (ETAR) on SMCs and endothelin receptor B (ETBR) on both SMCs and ECs. In PAH patients, plasma ET-1 is elevated and correlates with the severity and prognosis of the disease (Rubens et al., 2001). Particularly, ET-1 is overexpressed in PAECs and in plexogenic lesions (Giaid et al., 1993). Hence, ERA became one of the three main types of drug in current treatments. However, efficacy of ERA is limited in patients with CTD-PAH, especially SSc-PAH, which possesses a high level of inflammatory components such as increased IL-6 production (Hassoun et al., 2009; Itoh et al., 2006), revealing the governor role of inflammation in regulating several pathways including ET-1 in these patients. We therefore have

hypothesized that IL-6 may be upstream of the ET-1 system and regulates ET-1 signaling in the severe PAH.

MATERIALS AND METHODS

Reagents

The following antibodies were used: Purified rat-anti-mouse Mac-3 (cat. 550292), purified rat-anti-mouse CD31 (cat. 550274) (BD Pharmingen), HIF-1α (cat. NB100-479) (Novus Biologicals), rabbit anti PCNA (cat. ab29), rabbit anti IL-6 (cat. ab6672), rabbit anti VEGF-R2 (cat. ab2349) (Abcam), rat anti mouse F4/80 (cat. MCA 497GA) (AbD Serotect), rabbit antibody von Willebrand factor (cat. A008202) (Dako Glostrup, Denmark), phosphorylated Smad3 (pSmad3) (cat. 9134S) (Cell Signaling), rabbit anti GAPDH (cat. G9545), αSMA (cat. A2547&F3777) (Sigma), Bcl-2 (cat. sc-7383), phosphorylated extracellular signal-regulated kinases (pERK1/2) (cat. sc-7383), C-Jun N-terminal kinase (pJNK) (cat. sc-6254), JNK (cat. sc-571) (Santa Cruz), and endothelin A receptor (ETAR) (cat. ARE-001) (Alemone Labs). Vascular endothelial growth factor receptor (VEGF-R) inhibitor (SU5416) (cat. 13342) was purchased from Cayman Chemical Co. Recombinant human interleukin-6 (rhIL-6) (cat. 7270-IL-025/CF) was bought from R&D Systems.

Experimental procedure for the development of a model of severe mouse PAH

All animal procedures were performed in accordance with the Guidelines for animal experimentation established by the Kobe University Graduate school of Medicine, Japan. Mice were kept in a room with controlled temperature (22-24^{o}C) under a 12-hour-light-dark cycle. Food and water were accessible *ad libitum*. The experimental design was modified from that of

Ciuclan et al. (2011). Briefly, 3-week-old male SV129 wild-type mice (n=5-6 each group) received 20 mg/kg VEGF-R inhibitor (SU5416) (Hypoxia+SU), which was suspended in CMC [0.5% (w/v) carboxymethylcellulose sodium, 0.9% (w/v) sodium chloride, 0.4% (v/v) polysorbate 80, 0.9% (v/v) benzyl alcohol in deionized water] or vehicle (CMC only) (Hypoxia) subcutaneously three times a week and were exposed to chronic normobaric hypoxia (10% O_2) in a ventilated chamber for three weeks. The chamber was flushed with a mixture of room air and nitrogen and was opened on the alternate day during 20 min for injection, hygiene and feeding reason. The gas was recirculated. The hypoxic condition was monitored using an oxygen monitor (Fujikura, Japan). Control mice (Normoxia) were kept in the same room, under the same light-dark cycle.

Hemodynamic Measurements

Each mouse was anesthetized by isoflurane (1.4 mg/kg) inhalation via face mask. Isoflurane gas machine was connected to room air for normoxic mice or hypoxic chamber for hypoxic and hypoxia+SU mice. To evaluate pulmonary arterial pressure (PAP), 10 min after inhalant anesthesia, the right ventricle was assessed at subxiphoid site by a percutaneously inserted 25G needle connected to a pressure transducer. Right ventricular systolic pressure (RVSP) and heart rate (HR) were recorded on a Macintosh computer using the MacLab system (Bioresearch Center). The results were exploited if the HR under these conditions ranged between 300 and 500 beats per minute (bpm). After hemodynamic measurements, the chest was opened and the lung and heart were cleared of blood with phosphate buffered saline (PBS) via RV using 26G needle connected to a perfusion machine in constant pressure pump. Lung tissues were collected for histological and molecular profiling. The heart was removed. The RV was dissected from the

left ventricle (LV) and septum (S), then the Fulton index (RV/LV+S) and RV mass [RV (mg)/body weight (g) (BW)] were determined.

Histology, Immunohistochemistry (IHC) and Immunofluorescence (IF)

The right lung (RL) was removed after tight suturing at the hilus and snap-frozen for molecular profiling assays. The left lung (LL) was inflated with 0.1 ml of 4% paraformaldehyde (PFA) through a cathlon 22G inserted into trachea and pumped with constant pressure. Cathlon was released and trachea was closely tied, then the LL was removed, fixed in 4% PFA overnight and processed into paraffin using a standard procedure. Transverse section was performed to divide the LL into four pieces which were arranged in sequence and embedded in the same paraffin cassette and cut at 4 μm thickness. Five LLs in each group and 8 sections of each lung were investigated.

Lung specimens were de-paraffinized in a series of xylene baths. The slides were then rehydrated in graded ethanol and distilled water. To retrieve antigenicity, the tissue sections were incubated in trypsin 0.02% in 1xTBS for 8 min at 37^{o}C for IL-6 or heated using microwave in 10 mM citrate buffer (pH 6.0) 15 min for the others.

For IHC: After cooling in room temperature (RT) for 30 min, the sections were washed with PBS and immersed in PBS containing 3% hydrogen peroxide (H_2O_2) for 5 min and blocked with 5% bovine serum albumin (BSA) in PBS for 20 min. Primary antibody was applied and incubated at 4^{o}C overnight. For Mac3 staining, slides were blocked in 0.3% H_2O_2/40% Methanol/PBS for 1 h at RT. Following PBS washing, secondary antibody was applied 1 h at RT. 3,3 '-diaminobenzidine (DAB) was used as a chromogen (Dako, Carpinteria, CA).

For IF: The sections were washed with 0.05% Triton X in PBS (PBS-T) and blocked with 3% BSA/PBS-T for 20 min. Primary antibody was used at 4^{o}C overnight. Following PBS-T washing,

secondary antibody was applied at RT for 1 h protected from light. DAPI was added for 15 min for nuclei staining. Slides were incubated in autofluorescent-blocking reagent (CuSO4) for 60 min and mounted.

Image analysis

Slides were examined using Keyence BIOZERO microscope (Keyence, Osaka, Japan). Each group included 5 mice, 8 sections per mouse were checked. In each section around 40 small PA (< 100 μm diameter) sections were blindly evaluated. For muscularization quantification, the intensity of muscularization of small PA was determined based on the circumferential staining of α-smooth muscle actin (SMA) as either non-muscularized (N) (when no or little SMA staining) or partially muscularized (P) (when < 75% SMA staining) or fully muscularized (F) (when ≥ 75% SMA staining), then the percentage distribution of each calculated per group. The results were the mean of all. For PCNA quantification, the number of PCNA positive cells on the endothelial layer was manually scored. Macrophages were manually counted by two independent investigators using 400 x magnifications. A minimum of 40 fields/section or 40 small PA/section was examined. Results were presented as mean of macrophages/field or macrophages/vessel.

Quantitative real-time reverse transcription polymerase chain reaction (RT-PCR)

Total mRNA was isolated from RL tissue using Trizol reagent (Invitrogen) according to manual instruction and reversed transcribed using ReverTra Ace (Toyobo). 10ng cDNA was applied for real time polymerase chain reaction (RT-PCR) using Thunderbird SYBR qPCR Mix (Toyobo) with the Rotor-Gene Q Real Time PCR Systems (Qiagen, Germany). Specificity of amplified RT-PCR product was verified by melting curve analysis or agarose gel electrophoresis. Relative mRNA levels were analyzed with a quantitative comparative Ct method and normalized with

GAPDH or 18S gene expression as internal control. The primers used in this experiments were listed in table 1.

Immunoblotting

Frozen RL were minced and homogenized in RIPA buffer containing protease inhibitor cocktail. The lysates were eluted with 1x Laemmli buffer and resolved on SDS-PAGE gel, transferred to Immobilon polyvinylidene difluoride membrane (Millipore, Bedford, MA). Membranes were blocked with 5% skim milk in Tris-buffered saline-Tween 20 (TBS-T) at RT for 1 h and incubated with the primary antibody in Can Get Signal solution (Toyobo) at 4^{o}C overnight**.** Membranes were then washed 3 times with 1x TBS-T and incubated with the 2^{nd} antibody in Can Get Signal solution for 1 h at RT. The band was detected by using the Luminata Forte Western HRP Substrate (Millipore) and luminescence was observed on an ImageQuant LAS 4000 (GE, Japan). The membranes were then stripped with a solution containing SDS 1% and glycine 0.2% (pH=2) for 45 min at 50^{o}C and GAPDH was stained. Bands were quantified with AlphaEaseFC software (Alpha Innotech Corporation) and normalized with GAPDH.

Generating of primary pulmonary endothelial cells (pmPECs)

Preparation of antibody-coated beads

Sheep anti-rat IgG Dynabeads (cat. 110.35) (Invitrogen) was washed 6 times with sterile 0.1% BSA/PBS and resuspended at 80 millions beads/ml. Each wash was performed by sitting the beads on magnetic particle concentrator (MPC) (DynaMg-2 cat.12321D) (Invitrogen) for 1 min to allow the beads to sediment. Beads were then saturated with 10µl of Purified Rat-anti Mouse CD31 (CD-31) antibody. Coating was performed on a rotator standing at RT for 2 h. Beads were then washed 5 times as described above and resuspended in 200µl 0.1% BSA/PBS.

Magnetic bead sorting to isolate endothelial cells from young murine lung

Each 3 week-old mouse was anesthetized with pentobarbital (Kyoritsu-Seiyaku, Tokyo, Japan) and the thoracic cavity was assessed. The individual lung lobes (without the bronchi and surrounding connective tissue) were aseptically excised and immersed in ice-cold DMEM. The lobes were removed from the DMEM, finely minced by cutting around 100 times and then incubated with 15ml warm 0.1% collagenase/dispase solution in DMEM for enzymatic digestion for 45 min at 37^{o}C on a rotator. After the 45 min incubation, the digested tissue suspension was transferred into a 20ml syringe attached to a 14G cannula and homogenized around 12 times into a single cell suspension. The resulting cell suspension was filtered through a 40-µm strainer and washed with 15ml isolation media (IM) (20% FBS/DMEM and 1x Penicillin/Streptomycin) to stop digestion. The filtered cell suspension was centrifuged for 5 min at 400g. After removal of the supernatant, the cell pellet was resuspended in 3ml 0.1% BSA/PBS; 22.5 µl prepared magnetic beads coated with anti-CD31 antibodies was added and mixed at RT for 12 min. The bead was then sedimented using the MPC for 1 minute. After the removal of the supernatant, the cell pellet was washed 5 times with 3ml of 0.1% BSA/PBS, each time remounted on the MPC and then resuspended and mixed well in 3ml of HuMedia EG2 medium (cat. KE-2510S) (Kurabo, Japan) with FBS 2% and growth factors and 1x penicillin/streptomycin (VL) and plated into a 2% gelatin-coated 10cm disk. Total volume was brought to 10ml with VL in each disk. The alternating day, half of the medium was changed. The cells were cultured for an additional of 3-4 days to reach 70-80% confluence.

Resorting with magnetic beads coated anti-CD31 antibodies

At the confluence of 70 to 80%, the cells were detached by 0.05% Trypsin/EDTA for 3 min. When cells were completely detached, 2ml of IM was added to inhibit trypsinization. Cell suspension was spin down for 5 min at 400g and cell pellet was resuspended in 2ml 0.1 %

BSA/PBS. 10 µl prepared magnetic beads coated with anti-CD31 antibodies was added and rotated at room temperature for 12 min. Cells were washed 5 times with 0.1% BSA/PBS, each time mounted on MPC. Cells were then plated into a 2% gelatin-coated 10cm disk. The purity of pmPECs was determined using double immunofluorescent staining for CD31 and S100A4 (fibroblast marker).

Cell culture

Activated macrophages transformed from human monocytic cell line (THP-1 cat. RCB1189) and mouse pancreatic endothelial cell line (MS1) were obtained from RIKEN Cell Bank and cultured at 37^{o}C (5% CO2 and 95% air). THP-1 was cultured in RPMI Medium 1640 (Gibco) with 10% FBS. The experiment in vitro was carried out by culturing human macrophages transformed from THP-1under phorbol myristate acetate treatment (PMA) and then treating them in Hypoxia (1% O_2) combined with SU5416 (15nM) for 24 h. The cells were collected and mRNA and protein IL-6 expression were checked. MS1 cells were cultured in complete medium consisting DMEM/high glucose (cat. D5796) (Sigma) with 10% FBS. pmPECs were established in the lab as stated above and cultured with VL medium. The cells were subcultured by 0.05% trypsin (Gibco). MS1 cells and pmPECs were subjected to 50ng/ml IL-6 treatment for 24 h. The cells were collected and mRNA expression of ET-1 and ETBR were checked.

Proliferation assay

To assess the cell viability, MS1 were seeded at a concentration at 1x10^4 cells/well (96-well plate) and cultured in the incubator (5% CO_2 and at 37°C) in a normal medium as describe above. 24 h after seeding, the cells were starved using DMEM/High Glucose 0.2% FBS during 24 h. The cells were then treated with 50ng/ml IL-6 for 24 h. The cell viability was examined using the Cell Counting Kit WST-1 (cat. 345-06463) (Dojindo) according to the manufacturer's protocol.

Briefly 10µl of cell counting solution was added to each well, mixed and the cells were reincubated in incubator (5% CO_2 and at 37°C). The formazan-dyes were detected by measuring the absorbance at 450 nm (reference wavelength 655 nm) after 1h, 2h and 4h.

Data Analysis

Results are presented as the mean ± SEM. The data distribution was tested using Kolmogorov-Smirnov test. Normally distributed variables were analyzed by using an unpaired Student *t* test for direct 2-group comparisons and the post hoc Turkey test after a significant 1-way ANOVA *F* test for 3-group comparisons to identify which group differences accounted for significant overall ANOVA results. Variables not normally distributed were analyzed using nonparametric analysis with Kruskal-Wallis followed by Mann-Whitney *U test*. Statistical analysis was performed with the GraphPad Prism software package. $P < 0.05$ was considered significant.

RESULTS

Experimental model of severe PAH

SU5416 aggravated the elevated PAP and RV hypertrophy created by hypoxic condition

The murine model of severe PAH has been established by Ciuclan et al in 2011 (Ciuclan et al., 2011) by treating adult C57/Bl6 mice with SU5416 in chronic hypoxic environment. However, others have failed to reproduce this model (Gomez-Arroyo et al., 2012). Therefore, we aimed to modify the procedure by using young SV129 mice with higher frequency of treatment with SU5416. After 3 weeks, a clear decrease in body weight was observed in Hypoxia+SU mice in

comparison with Hypoxia ($P < 0.05$) and Normoxia ($P < 0.01$) mice. There was no significant difference between Hypoxia and Normoxia mice (Table 2).

We observed an upregulation of cleaved caspase-3 in Hypoxia+SU group ($P< 0.01$ vs. Normoxia or Hypoxia), indicating an increased apoptosis (Figure 1B). Chronic hypoxia induced the elevation of RVSP in mice with either SU5416 or vehicle, compared with the mice under normoxia (RVSP=37mmHg; 29mmHg and 22.5mmHg; respectively). Importantly, treating with SU5416 induced a further increase of RVSP (Figure 1C). A RV hypertrophy was noted in Hypoxia (Fulton index, 0.40; RV/BW, 1.3; $P < 0.01$ vs. Normoxia, 0.31; 1.1) and was further elevated in Hypoxia+SU (Fulton index, 0.55; RV/BW, 1.8; $P< 0.001$ vs. Hypoxia) (Figure 1D, E).

SU5416 augmented the muscularization of distal acinar arterioles and the thickening of arteriolar medial layer generated by hypoxia

One characteristic of PAH is the muscularization of distal acinar arterioles. While the majority of normal lung small vessels was non-muscularized (N) (68%) and only a small number of fully muscularized (F) was noted (12%), Hypoxia and Hypoxia+SU mice showed a reduction in N percentage (53% and 32%, respectively), along with the elevation of F percentage (24% and 42%, respectively) after 3 weeks. Combination of SU5416 and hypoxia profoundly enhanced the degree of F ($P< 0.0001$ vs. Hypoxia) and decreased the level of N ($P< 0.0001$ vs. Hypoxia) (Figure 2B).

Only SU5416 combined with hypoxia can cause plexogenic lesions

To investigate the remodeling of small PA, we performed IHC of von Willebrand factor (vWF), an endothelial cell marker and double IF staining for vWF and SMA (Figure 2A). Histological examination revealed various degrees of concentric neointimal thickness in pulmonary arterioles,

particularly the complete lumen obliteration by multiple layers of cells expressing vWF in Hypoxia+SU group (Figure 2Ac,f). On the contrary, no neointimal thickening lesions were observed and the endothelium still maintained monolayer in hypoxic and normoxic mice (Figure 2Ab,d,e).

Proliferative endothelial cells completely occluded the small lung arteries in hypoxia combined SU5416-treated mice

To demonstrate whether the cells expressing vWF in plexogenic lesions were proliferating cells, we performed double IF staining for the proliferation marker proliferating-cell nuclear antigen (PCNA) and vWF. Cells expressing vWF in neointimal thickening lesions in pulmonary arterioles of Hypoxia+SU mice remarkably up-regulated PCNA contributing to plexogenic lesion formation (Figure 3Ac), whereas, that of hypoxic and normoxic mice exhibited minimal PCNA expression (Figure 3Aa,b). A three time increase in the amount of PCNA positive cells in endothelium of remodeled arterioles was noted in Hypoxia+SU compared with Hypoxia and Normoxia ($P< 0.001$), whereas no significant difference between hypoxic and normoxic mice (Figure 3B).

Alteration of biomarkers, inflammatory profiles and signaling pathways in hypoxia combined SU5416-treated group

Biomarker analysis revealed that angio-occlusion in SU5416-treated mice under hypoxia was the consequence of hyper-proliferation and resistance to apoptosis

Since it has been previously showed that exposure to chronic hypoxia combined with VEGF-R inhibitor could generate an endothelial population which escaped from the apoptosis and became

aberrantly proliferative (Taraseviciene-Stewart et al., 2001, 2006), we sought to investigate this phenomenon in Hypoxia combined SU5416-treated mouse model. VEGF-A mRNA was elevated in Hypoxia alone ($P < 0.01$ vs. Normoxia) and further enhanced in Hypoxia+SU ($P < 0.05$ vs. Hypoxia) (Figure 3D). VEGF-R2 mRNA and protein levels were up-regulated in Hypoxia+SU ($P < 0.01$ vs. Normoxia) (Figure 3E, 3F), but were not enhanced in mice under hypoxia only (Figure 3E, 3F). mRNA of MMP-9 was increased in the hypoxic group ($P< 0.01$ vs. Normoxia) and further induced in Hypoxia+SU group ($P< 0.05$ vs. Hypoxia) (Figure 3C). In addition, we assessed the expression of pJNK and pERK1/2, which are known as growing factors for PAECs. Protein level of pJNK and pERK1/2 in the lung lysates were remarkably raised in Hypoxia+SU-treated mice ($P< 0.05$ vs. Hypoxia), while exposure to hypoxia only had no potent effect (Figure 3I, 3J). Furthermore, quantitative RT-PCR and immunoblot were performed for Bcl-2, an anti-apoptotic marker. Only Hypoxia+SU could increase mRNA and protein levels of Bcl-2 ($P< 0.05$ vs. Hypoxia) (Figure 3G, 3H).

Inflammatory profile altered in response to hypoxia with/without VEGF R inhibition

To explore the possibility that inflammatory cell infiltration may contribute to the formation of neointimal thickening and occluded arterioles, we performed IHC for Mac3 antibody, a macrophage marker, and quantified the number of macrophages in the lungs and in the adventitia of lung arterioles. Hypoxia induced recruitment of macrophages to the lungs and the adventitia of arterioles ($P< 0.01$ vs Normoxia) (Figure 4Aa,b,d,e; 4B; 4C). Hypoxia+SU further increased these numbers two to three times ($P< 0.0001$ vs. Hypoxia) (Figure 4Ab,c,e,f; 4B; 4C). The results were supported by Western blot data that F4/80 expression in lung lysates significantly enhanced under hypoxic exposure ($P< 0.05$ vs. Normoxia) and three times greater in hypoxia combined with SU5416 treatment ($P< 0.01$ vs. Hypoxia) (Figure 4D). Moreover, monocyte

chemotactic protein-1 (MCP-1), an important chemokine in recruitment and activation of macrophages, was also profoundly up-regulated in Hypoxia+SU only ($P< 0.001$ vs. Hypoxia and Normoxia) (Figure 4E).

IL-6 and its receptor were elevated in the lungs under hypoxia combined SU5416 treatment

To investigate the role of recruited macrophages in the adventitia of remodeled arterioles in the formation of plexogenic lesions, we concentrated on proinflammatory cytokine IL-6, being well known as one of the most important cytokines associated with PAH development. IHC (Figure 5A a-c) and double IF staining (Figure 5A d-i) were carried out for IL-6 or IL-6 and SMA, respectively. Combination of SU5416 and chronic hypoxia induced abundant IL-6 in the adventitia of remodeled arterioles (Figure 5Ac,f,i), whereas, hypoxia alone only generated minimal expression (Figure 5Ab,e,h). No detectable signal was observed in normoxic mice (Figure 5Aa,d,g). Immunoblot and quantitative RT-PCR also confirmed the greater up-regulation of protein and mRNA IL-6 in Hypoxia+SU ($P < 0.001$ and $P< 0.05$ vs. Hypoxia, respectively), while no significant increase was observed in hypoxic mice (P=0.3 and 0.14, vs. Normoxia, respectively) (Figure 5B, 5C). Similarly, IL-6 receptor mRNA was significantly raised in Hypoxia+SU mice ($P< 0.05$ vs. Hypoxia and Normoxia) only. (Figure 5D).

Hypoxia inducible factor (HIF-1α) signaling machinery, transforming growth factor β (TGF-β)/bone morphogenic protein (BMP)/Smad axis was perturbed in mice exposed to hypoxia combined with/without SU5416

As HIF-1α is known to be elevated in lung of patients with idiopathic PAH, we aimed to determine HIF-1α level. Western blot results described a marked elevation of HIF-1α protein in the lung of hypoxic mice ($P < 0.05$ vs. Normoxia) and this effect was further increased in Hypoxia+ SU group ($P < 0.01$ vs. Hypoxia) (Figure 6A). We assessed the gene expression of

TGF- β/BMP/Smad axis. TGF- β mRNA was up-regulated under hypoxic exposure ($P < 0.05$ vs. Normoxia), with no further influence created by SU5416 combination (Figure 6C). In contrast, protein level of phosphorylated Smad3, downstream component of TGF- β signaling which modulated cellular response linked to vascular remodeling, was slightly elevated in hypoxic treatment (P=0.4 vs. Normoxia) but six times greater promoted in Hypoxia+SU ($P < 0.05$) (Figure 6B). A significant reduction in BMPRII mRNA expression was noted in hypoxic mice ($P < 0.05$ vs. Normoxia), with no advanced effect in Hypoxia+SU mice (Figure 6D).

Disturbance in endothelin pathway under combination of chronic hypoxia and VEGF R inhibition

There was an increase in ET-1 and ETAR mRNA ($P< 0.01$ vs. Hypoxia and Normoxia) (Figure 7A, 7B) and a reduction in ETBR mRNA ($P< 0.05$ vs. Hypoxia; $P < 0.01$ vs. Normoxia) (Figure 7D) under combination treatment of hypoxia and SU5416, while, no influence of hypoxic treatment was noted in ET-1, ETAR and ETBR mRNA levels (Figure 7A, 7B, 7D). Similarly, ETAR protein was augmented in Hypoxia+SU-treated mice only (Figure 7C). Interestingly, immunostaining results depicted a colocalization of ETAR (red) and SMA (green) in the media of arterioles in Hypoxia+SU-treated mice only (Figure 7Ec,f). No colocalized signal in hypoxic and normoxic mice was recorded (Figure 7Ea,b,d,e).

In vitro influence of Hypoxia combined with SU5416 on IL-6 expression and effect of IL-6 on endothelin signaling pathway

Hypoxia combined with SU5416 promoted IL-6 expression in human macrophages

In cultured human macrophages, IL-6 mRNA and protein expression were increased in Hypoxia+SU-treated cells ($P < 0.05$ vs. Hypoxia; $P < 0.01$ vs. Normoxia), while exposure to hypoxia only enhanced slightly IL-6 protein (P=0.2 vs. Normoxia) (Figure 8).

Recombinant human IL-6 stimulated the proliferation and regulated ECs in increasing ET-1 and decreasing ETBR expression

In MS1 and pmPECs, IL-6 treatment (50ng/ml) increased ET-1 mRNA ($P< 0.05$ vs. controls) and reduced mRNA ETBR expression ($P< 0.05$; $P< 0.01$ vs. controls in MS1 and in pmPECs, respectively) (Figure 9). IL-6 treatment enhanced proliferation of MS1 cells ($P< 0.001$ vs. controls) detected by WST-1 assay (Figure 9C).

DISCUSSION

The newly optimized mouse model of severe PAH

The hallmark of severe PAH patients is the remodeling in small lung vessels characterized by concentric neointimal thickening, plexogenic lesions, recruitment of inflammatory cells, and distal arteriolar wall muscularization (Tuder et al., 1994). To date, several rat models of severe PAH closely mimicking human conditions have been established. The closest one combines hypoxia with a SU5416 treatment (Abe et al., 2010; Taraseviciene-Stewart et al., 2001). However, this model could not provoke the inflammatory response in the rat lung (Abe et al., 2010; Taraseviciene-Stewart et al., 2001), a common phenomenon observed in patients (Cool et al., 1997; Hall et al., 2009; Pinto et al., 2004; Tuder et al., 1994). It might explain the discrepancy in application of several drugs such as simvastatin (Taraseviciene-Stewart et al., 2006), which provides a good recovery in the rat model, yet shows no beneficial effects in

humans (Kawut et al., 2011). Problems have occurred in establishing the severe PAH in mouse, the common alternative to rats as laboratory animals. First, mice are less vulnerable to hypoxia than rats regarding pulmonary vessel remodeling (Dempsey et al., 2009; Frank et al., 2008; Nozik-Grayck et al., 2008). Hypoxia induces genes involved in EC proliferation in rats but not in mice (Hoshikawa et al., 2003). Second, the accumulation of SU5416 in lungs is less in mice. Higher systemic and renal clearance of SU5416 in mice was noted and SU5416 is hepatically metabolized by CYP450-1A, a cytochrome distinctly expressed in animal species (Martignoni et al., 2006; Nelson et al., 2004; Ye et al., 2006). Repeated administration of SU5416 induces several CYP450 in the liver, which differ between the two species (Craft et al., 2002; Martignoni et al., 2006). Ciuclan et al. successfully generated the severe PAH model from adult C57/Bl6 mice (Ciuclan et al., 2011). However, this protocol could not be reproduced in other workplaces (Gomez-Arroyo et al., 2012). Different mouse strains may react differently and younger mice with rapidly maturing lungs are more vulnerable when exposed to hypoxia (Stenmark et al., 2006). We thus used young SV129 mice, which were proven more sensitive to hypoxia than C57/Bl6 (Tada et al., 2008), and increased the frequency of SU5416 treatment.

Consistent with previous reports about the role of SU5416 in inducing a sustained death of pulmonary ECs (Ciuclan et al., 2011; Sakao et al., 2005; Taraseviciene-Stewart et al., 2001), we observed a marked increase of cleaved caspase-3 in our model. Hypoxia-induced inflammation (Burke et al., 2009; Savale et al., 2009) together with the apoptotic bodies from apoptotic ECs may stimulate the release of IL-6 and MCP-1 (Berda-Haddad et al., 2011; Curtis et al., 2009), which in turn, may recruit macrophages in the injured vessels, which might ultimately lead to the development of severe PAH.

IL-6 as a potential conductor in severe PAH

IL-6, an important proinflammatory cytokine in PAH progression, is produced by activated macrophages, fibroblasts, ECs and SMCs. Indeed, IL-6 is steadily increased and considered prognosis factor in idiopathic and inflammation-associated PAH (Humbert et al., 1995; Li et al., 2012; Nishimaki et al., 1999; Soon et al., 2010). Our study demonstrated an up-regulation of IL-6 in Hypoxia+SU, especially an abundance of IL-6 in the adventitia of remodeled arterioles. Consistently, IL-6 elevates in and around the angio-obliterating lesions in SU+ovalbumin rat PAH model (Mizuno et al., 2012). It is possible that IL-6 *per se* may stimulate the proliferation of SMCs and ECs (Steiner et al, 2009; Yao et al., 2006, 2007), and consequently form medial and concentric neointimal thickening and plexogenic lesions, the fingerprints of severe PAH (Tuder et al., 1994). Our experiments confirmed this idea by showing that 50ng/ml IL-6 stimulated the MS1 cell growth in vitro. IL-6 triggers ECs at a dose dependent manner, i.e. ≥ 50ng/ml IL-6 render cerebral ECs proliferative, but 25ng/ml IL-6 do not (Yao et al., 2006). In vivo, even though IL-6 is slightly elevated in hypoxic mice, neither arteriolar obliteration nor proliferative ECs was observed. This is consistent with previous studies indicating that hypoxia alone cannot generate proliferation of ECs (Steiner et al., 2009; Voelkel and Tuder, 2000; Yu and Hales, 2011). Hypoxia creates only a short-course raise of IL-6 peaking at day 7^{th} and returning to the baseline at day 14^{th} (Savale et al., 2007). IL-6 Tg^{+} mice also display most important features of severe PAH under hypoxia (Steiner et al., 2009). However, transgenic models do not fully mirror the human condition. In this model, the authors show that IL-6 genetic overexpression induced PAH is worsened by hypoxia. The IL-6 expression levels however were not measured, which makes difficult to establish how strong the development of PAH correlates with IL-6 or with hypoxia. Moreover, it is not clear whether IL-6 produced by Clara cells affects PA remodeling by directly targeting vessel wall cells or by indirect effects

mediated by inflammatory cells themselves. In the present study, we have shown that the worsening of the PAH by SU5416 treatment is associated with an increased expression of IL-6. Ciuclan et al. depicted an elevation of mRNA IL-6 and macrophages in the lung of their model, too (Ciuclan et al., 2011). Nevertheless, no relationship between macrophages, IL-6 and arteriolar remodeling had been cited. Using Mac3 marker, we described an accumulation of macrophages in the similar areas of IL-6 expression, which suggested that IL-6 may be secreted from adventitial macrophages of remodeled arterioles. This data was supported by our work in vitro indicating that macrophages produced increased IL-6 under hypoxia combined with SU5416.

Enormous infiltration of macrophages is often mentioned within and around the remodeled arterioles in severe PAH. Macrophages directly release MMP-9 (Mautino et al., 1999) and MCP-1 (Yoo et al., 2005; Yoshimura et al., 1989), which, as a positive feedback, recruit macrophages (Taylor et al., 2006). In mice, combination of MMP-9 overexpression and monocrotaline administration generates PAH with occluded precapillary vessels and sustained macrophage infiltration (George et al., 2012). In vitro, increased MMP-9 by IL-6 causes ECs and SMCs to proliferate (Yao et al., 2006, 2007). MCP-1 is depicted in ECs, SMCs, and macrophages within remodeled arterioles and closely associated with pulmonary vascular resistance in PAH patients (Kimura et al., 2001). MMP-9 and MCP-1 are also secreted by ECs (Genersch et al., 2000; Kimura et al, 2001; Sanchez et al., 2007; Yao et al., 2006) in PAH. Therefore, their high level in Hypoxia+SU may result from the overproduction of proliferative ECs, which in turn contributing to the recruitment and migration of macrophages (Sanchez et al., 2007).

IL-6 moderates hyperproliferation and anti-apoptosis of ECs through VEGF, MAPK signaling and Bcl-2. VEGF and VEGF-R2 are the key components for EC survival and high levels of them have been found in the lung, particularly in plexogenic lesions of PAH patients (Tuder RM et al., 1994). VEGF and VEGF-R2 are up-regulated by IL-6 and trigger proliferation of ECs via pERK1/2. Consistently, blocking VEGF or VEGF-R2 abolishes IL-6-induced proliferation (Steiner et al., 2009; Yao et al., 2006). JNK, another MAPK component, is not only an anti-apoptosis but a proliferative factor as well (Ma et al., 2012). Activation of pJNK induces prosurvival signaling in ECs (Salameh et al., 2005), increases the proliferation and decreases the apoptosis of bovine PAECs (Ma et al., 2012). We therefore examined protein levels of VEGF-R2, pERK1/2 and pJNK in our model and recorded the elevation of all these parameters in Hypoxia+SU. In PAH patients, Bcl-2 is increased in the lungs (Geraci et al., 2001) and in PAECs associated with irreversibility of the disease (Lévy et al., 2007). Furthermore, Bcl-2 is increased in IL-6 Tg^{+} mice (Steiner et al., 2009) and induced by VEGF in serum-starved ECs (Cai et al., 2003; Gerber et al., 1998). In our model, Bcl-2 could be indirectly induced by IL-6 through VEGF to create an overproliferative EC population.

HIF-1α, another IL-6-regulated factor, is highly expressed in angio-obliterative proliferative lesions in PAH patients (Tuder et al., 2001a). We noted a positive correlation between IL-6 and HIF-1α in Hypoxia and Hypoxia+SU, while no association between them was observed in Ciuclan's study (Ciuclan et al., 2011). The further augmentation of HIF-1α in Hypoxic+SU mice may be partly induced by the activation of IL-6/Stat3/HIF-1α axis, an important pathway in cancer cells (Grivennikov et al., 2009; Lang et al., 2007; Nilsson et al., 2010), and mentioned in rats with severe PAH (Mizuno et al., 2012). IL-6 triggers phosphorylation of Stat3 (Heikkila et al., 2008), leading to up-regulation of HIF-1α either by blocking its degradation or elevating its

synthesis (Jung et al., 2005). Interestingly, activation of Stat3 by IL-6 mediates expression of miR-17/92, resulting to the repression of BMPRII protein (Brock et al., 2009), an important inhibitor of EC and SMC proliferation. The translational interference of IL-6 to BMPRII explains the difference only at the protein level of BMPRII but not at the mRNA between Hypoxia and Hypoxia+SU.

IL-6 potentially regulated endothelin signaling in severe PAH

IL-6 enhances TGF-β-dependent Smad3 signaling (Zhang et al., 2005). pSmad3 potentiates TGF-β-induced ET-1 from ECs (Castanares et al., 2006; Rodríguez-Pascual et al., 2003, 2004). We demonstrated that the increased TGF-β expression in Hypoxia and Hypoxia+SU was not different, but pSmad3 expression was elevated only in the latter group, which might indicate that pSmad3 contributed to the elevation of ET-1 expression.

ETAR and ETBR on the SMCs mediate the vasoconstriction and proliferation of vascular SMCs (Davie et al., 2002; Kedzierski and Yanagisawa, 2001; Levin, 1995), while ETBR on the ECs induces the release of vasodilator and anti-proliferative modulators. Furthermore, ETBR participates in the clearance of ET-1 from the lungs and inhibition of endothelin converting enzyme-1 (ECE-1) (Fukuroda et al., 1994; Naomi et al., 1998). In patients with PAH, ET-1 plasma levels are elevated and correlated with the severity and prognosis of the disease (Rubens et al., 2001). ET-1 is particularly overexpressed in plexogenic lesions and PAECs (Giaid et al., 1993). Similarly, we observed a high level of ET-1 mRNA in Hypoxia+SU. However, in hypoxia alone, ET-1 did not change. Several researches indicate the positive (Kourembanas et al., 1993; Perrella et al, 1992) or negative/neutral (Markewitz et al., 1995) effect of hypoxia on ET-1 production. One reason cited by those authors to explain the negative/neutral effect is the inhibitive role of nitric oxide (NO) on ET-1 production of ECs. In hypoxic mice, we also

observed the increase of endothelial NO synthase (eNOS) gene expression in the hypoxic group (data not shown). In addition, we observed an upregulation of ETAR mRNA and protein in Hypoxia+SU. Immunofluorescence revealed the presence of ETAR on the SMCs, only in Hypoxia+SU. Moreover, in vitro, IL-6 raised the mRNA ET-1 in pmPECs and MS1, consistent with previous report showing that IL-6 is a potent stimulator of ET-1 production by EC (Kahaleh and Fan, 1997). This effect is dose dependent (Kahaleh and Fan, 1997), because low dose of IL-6 (0.5-10ng/ml) has no effect on ECs of the aorta, PA, and retinal microvessels on the release of ET-1 (Kanse et al., 1991). This is consistent with our results in mice under hypoxia alone showing slightly elevated IL-6 and hence no change of ET-1. The up-regulation of both ET-1 and ETAR may activate ERK1/2 inducing SMC proliferation (Chen et al., 2009; Yogi et al., 2007; Zhang et al., 2003). Furthermore, we noted ETBR reduction in vitro and in vivo. We have measured ET-1 expression at the mRNA level only. Nevertheless, we can speculate that the reduced ET-1 clearance and ECE-1 inhibition consequent to a reduction of ETBR expression might potentiate ET-1 peptide abundance in lungs of Hypoxia+SU mice. Since ETBR expression in SMC increases in PAH (Bauer et al., 2002), the overall reduction of ETBR that we observed might be underestimated in the ECs, which implies that the vasodilation and antiproliferation mediated by ETBR on ECs might be particularly down-regulated. This also might explain why selective ETAR antagonist is not superior to non-selective ERA in human PAH treatment (Benza et al., 2006; Christian et al., 2008).

CONCLUSION

We have optimized a model of severe PAH by using young SV129 mice and a combination of hypoxia and sustained VEGF-R inhibition. These mice exhibited most important characteristics

of severe PAH observed in humans: concentric neointimal wall thickening, plexogenic lesions, recruitment of macrophages, and distal arteriolar wall muscularization. Using this model, we have demonstrated the role of adventitia-derived IL-6 and recruited macrophages in adventitia of remodeled vessels in the development of plexogenic lesions, suggesting IL-6 in the adventitia as a potential therapeutic target. Moreover, we produced evidences for a potential regulation of ET-1 signaling by IL-6 in the development of severe PAH. The cells in plexogenic sites were proliferative ECs with high expression of VEGF, VEGF-R2, Bcl-2, and HIF-1α, inferring the cancer-like features of PAH with excess proliferation and impaired apoptosis. These results may explain the difficulties in treatment of severe human PAH with available drugs. Therefore, this model can be reliable in investigating pathophysiological mechanisms and testing new medications for treating severe PAH patients.

ACKNOWLEDGMENTS

This work was supported by JSPS KAKENHI (23590123) Grant-in-Aid for Scientific Research (C) to N.E.

H.T.V. is a recipient of a scholarship from Rotary Yoneyama Memorial Foundation.

REFERENCES

Abe K, Toba M, Alzoubi A, Ito M, Fagan KA, Cool CD, et al. Formation of Plexiform Lesions in Experimental Severe Pulmonary Arterial Hypertension. Circulation. 2010;121:2747-54.

Archer SL, Weir EK, Wilkins MR. Basic Science of Pulmonary Arterial Hypertension for Clinicians: New Concepts and Experimental Therapies. Circulation. 2010;121:2045-66.

Bauer M, Wilkens H, Langer F, Schneider SO, Lausberg H, Schafers H-J. Selective Upregulation of Endothelin B Receptor Gene Expression in Severe Pulmonary Hypertension. Circulation. 2002;105:1034-6.

Benza RL, Frost A, Girgis R, Langleben D, Lawrence EC, Naeije R. Chronic treatment of pulmonary arterial hypertension (PAH) with sitaxentan and bosentan [abstract]. Proc Am Thorac Soc. 2006;3:A729.

Berda-Haddad Y, Robert S, Salers P, Zekraoui L, Farnarier C, Dinarello CA, Dignat-George F, Kaplanski G. Sterile inflammation of endothelial cell-derived apoptotic bodies is mediated by interleukin-1β. Proceedings of the National Academy of Sciences. 2011;108:20684-9.

Brock M, Trenkmann M, Gay RE, Michel BA, Gay S, Fischler M, et al. Interleukin-6 Modulates the Expression of the Bone Morphogenic Protein Receptor Type II Through a Novel STAT3-microRNA Cluster 17/92 Pathway. Circulation Research. 2009;104:1184-91.

Burke DL, Frid MG, Kunrath CL, Karoor V, Anwar A, Wagner BD, et al. Sustained hypoxia promotes the development of a pulmonary artery-specific chronic inflammatory microenvironment. American Journal of Physiology - Lung Cellular and Molecular Physiology. 2009;297:L238-L50.

Cai J, Ahmad S, Jiang WG, Huang J, Kontos CD, Boulton M, et al. Activation of Vascular Endothelial Growth Factor Receptor-1 Sustains Angiogenesis and Bcl-2 Expression Via the Phosphatidylinositol 3-Kinase Pathway in Endothelial Cells. Diabetes. 2003;52:2959-68.

Castanares C, Redondo-Horcajo M, Magan-Marchal N, Lamas S, Rodriguez-Pascual F. Transforming Growth Factor-beta Receptor Requirements for the Induction of the Endothelin-1 Gene. Experimental Biology and Medicine. 2006;231:700-3.

Chen Q.-w., Edvinsson L., Xu C.-B. Role of ERK/MAPK in endothelin receptor signaling in human aortic smooth muscle cells. BMC Cell Biology C7 - 52. 2009;10:1-13.

Christian FO, Ralf E, Wilhelm Kirch, and David Pittrow. Inhibition of endothelin receptors in the treatment of pulmonary arterial hypertension: does selectivity matter? European Heart Journal 2008;29:1936-48.

Ciuclan L, Bonneau O, Hussey M, Duggan N, Holmes AM, Good R, et al. A Novel Murine Model of Severe Pulmonary Arterial Hypertension. American Journal of Respiratory and Critical Care Medicine. 2011;184:1171-82.

Condliffe R, Kiely DG, Peacock AJ, Corris PA, Gibbs JSR, Vrapi F, et al. Connective Tissue Disease-associated Pulmonary Arterial Hypertension in the Modern Treatment Era. American Journal of Respiratory and Critical Care Medicine. 2009;179:151-7.

Cool CD, Kennedy D, Voelkel NF, Tuder RM. Pathogenesis and evolution of plexiform lesions in pulmonary hypertension associated with scleroderma and human immunodeficiency virus infection. Human Pathology. 1997;28:434-42.

Craft ES, DeVito MJ, Crofton KM. Comparative Responsiveness of Hypothyroxinemia and Hepatic Enzyme Induction in Long-Evans Rats Versus C57BL/6J Mice Exposed to TCDD-like and Phenobarbital-like Polychlorinated Biphenyl Congeners. Toxicological Sciences. 2002;68:372-80.

Curtis AM, Wilkinson PF, Gui M, Gales TL, Hu E, Edelberg JM. p38 mitogen-activated protein kinase targets the production of proinflammatory endothelial microparticles. Journal of Thrombosis and Haemostasis. 2009;7:701-9.

Davie N, Haleen SJ, Upton PD, Polak JM, Yacoub MH, Morrell NW, et al. ETA and ETB Receptors Modulate the Proliferation of Human Pulmonary Artery Smooth Muscle Cells. American Journal of Respiratory and Critical Care Medicine. 2002;165:398-405.

Dempsey EC, Wick MJ, Karoor V, Barr EJ, Tallman DW, Wehling CA, et al. Neprilysin Null Mice Develop Exaggerated Pulmonary Vascular Remodeling in Response to Chronic Hypoxia. The American Journal of Pathology. 2009;174:782-96.

Fisher MR, Mathai SC, Champion HC, Girgis RE, Housten-Harris T, Hummers L, et al. Clinical differences between idiopathic and scleroderma-related pulmonary hypertension. Arthritis & Rheumatism. 2006;54:3043-50.

Frank DB, Lowery J, Anderson L, Brink M, Reese J, de Caestecker M. Increased susceptibility to hypoxic pulmonary hypertension in Bmpr2 mutant mice is associated with endothelial dysfunction in the pulmonary vasculature. American Journal of Physiology - Lung Cellular and Molecular Physiology. 2008;294:L98-L109.

Fukuroda T, Fujikawa T, Ozaki S, Ishikawa K, Yano M, Nishikibe M. Clearance of Circulating Endothelin-1 by ETB Receptors in Rats. Biochemical and Biophysical Research Communications. 1994;199:1461-5.

Genersch E, Hayess K, Neuenfeld Y, Haller H. Sustained ERK phosphorylation is necessary but not sufficient for MMP-9 regulation in endothelial cells: involvement of Ras-dependent and -independent pathways. Journal of Cell Science. 2000;113:4319-30.

George J, Sun J, D'Armiento J. Transgenic expression of human matrix metalloproteinase-1 attenuates pulmonary arterial hypertension in mice. Clinical Science 2012; 122:83-92.

Geraci MW, Moore M, Gesell T, Yeager ME, Alger L, Golpon H, et al. Gene Expression Patterns in the Lungs of Patients With Primary Pulmonary Hypertension: A Gene Microarray Analysis. Circulation Research. 2001;88:555-62.

Gerber HP, Dixit V, Ferrara N. Vascular Endothelial Growth Factor Induces Expression of the Antiapoptotic Proteins Bcl-2 and A1 in Vascular Endothelial Cells. Journal of Biological Chemistry. 1998;273:13313-6.

Giaid A, Yanagisawa M, Langleben D, Michel RP, Levy R, Shennib H, et al. Expression of Endothelin-1 in the Lungs of Patients with Pulmonary Hypertension. New England Journal of Medicine. 1993;328:1732-9.

Girgis RE, Mathai SC, Krishnan JA, Wigley FM, Hassoun PM. Long-Term Outcome of Bosentan Treatment in Idiopathic Pulmonary Arterial Hypertension and Pulmonary Arterial Hypertension Associated with the Scleroderma Spectrum of Diseases. The Journal of Heart and Lung Transplantation. 2005;24:1626-31.

Golembeski SM, West J, Tada Y, Fagan KA. INterleukin-6 causes mild pulmonary hypertension and augments hypoxia-induced pulmonary hypertension in mice*. CHEST Journal. 2005;128:572S-3S.

Gomez-Arroyo J, Saleem SJ, Mizuno S, Syed AA, Bogaard HJ, Abbate A, et al. A brief overview of mouse models of pulmonary arterial hypertension: problems and prospects. American Journal of Physiology - Lung Cellular and Molecular Physiology. 2012;302:L977-L91.

Grivennikov S, Karin E, Terzic J, Mucida D, Yu G-Y, Vallabhapurapu S, et al. IL-6 and Stat3 Are Required for Survival of Intestinal Epithelial Cells and Development of Colitis-Associated Cancer. Cancer Cell. 2009;15:103-13.

Hall S, Brogan P, Haworth SG, Klein N. Contribution of inflammation to the pathology of idiopathic pulmonary arterial hypertension in children. Thorax. 2009;64:778-83.

Hassoun PM, Mouthon L, Barbera JA, Eddahibi S, Flores SC, Grimminger F, et al. Inflammation, Growth Factors, and Pulmonary Vascular Remodeling. Journal of the American College of Cardiology. 2009;54:S10-S9.

Heikkila K, Ebrahim S, Lawlor DA. Systematic review of the association between circulating interleukin-6 (IL-6) and cancer. European Journal of Cancer. 2008;44:937-45.

Hoshikawa Y, Nana-Sinkam P, Moore MD, Sotto-Santiago S, Phang T, Keith RL, Morris KG, Kondo T, Tuder RM, Voelkel NF, Geraci MW. Hypoxia induces different genes in the lungs of rats compared with mice. Physiol Genomics 2003 Feb 6;12(3):209-19. 2003.

Humbert M, Monti G, Brenot F, Sitbon O, Portier A, Grangeot-Keros L, et al. Increased interleukin-1 and interleukin-6 serum concentrations in severe primary pulmonary hypertension. American Journal of Respiratory and Critical Care Medicine. 1995;151:1628-31.

Humbert M, Sitbon O, Simonneau Gr. Treatment of Pulmonary Arterial Hypertension. New England Journal of Medicine. 2004;351:1425-36.

Itoh T, Nagaya N, Ishibashi-Ueda H, Kyotani S, Oya H, Sakamaki F, et al. Increased plasma monocyte chemoattractant protein-1 level in idiopathic pulmonary arterial hypertension. Respirology. 2006;11:158-63.

Jung JE, Lee H-G, Cho I-H, Chung DH, Yoon S-H, Yang YM, et al. STAT3 is a potential modulator of HIF-1-mediated VEGF expression in human renal carcinoma cells. The FASEB Journal. 2005; 19(10):1296-8.

Kahaleh MB, Fan PS. Effect of cytokines on the production of endothelin by endothelial cells. Clin Exp Rheumatol. 1997;15(2):163-7.

Kanse SM, Takahashi K, Lam H-C, Rees A, Warren JB, Porta M, et al. Cytokine stimulated endothelin release from endothelial cells. Life Sciences. 1991;48:1379-84.

Kawut SM, Bagiella E, Lederer DJ, Shimbo D, Horn EM, Roberts KE, et al. Randomized Clinical Trial of Aspirin and Simvastatin for Pulmonary Arterial Hypertension: ASA-STAT. Circulation. 2011;123:2985-93.

Kawut SM, Taichman DB, Archer-Chicko CL, Palevsky HI, Kimmel SE. HEmodynamics and survival in patients with pulmonary arterial hypertension related to systemic sclerosis*. CHEST Journal. 2003;123:344-50.

Kedzierski RM, Yanagisawa M. Endothelin system: the double-edged sword in health and disease. Annu Rev Pharmacol Toxicol. 2001;41:851-76.

Kimura H, Okada O, Tanabe N, Tanaka Y, Terai M, Takiguchi Y, et al. Plasma Monocyte Chemoattractant Protein-1 and Pulmonary Vascular Resistance in Chronic Thromboembolic Pulmonary Hypertension. American Journal of Respiratory and Critical Care Medicine. 2001;164:319-24.

Kourembanas S, McQuillan LP, Leung GK, Faller DV. Nitric oxide regulates the expression of vasoconstrictors and growth factors by vascular endothelium under both normoxia and hypoxia. The Journal of Clinical Investigation. 1993;92:99-104.

Lang SA, Moser C, Gaumann A, Klein D, Glockzin G, Popp FC, et al. Targeting Heat Shock Protein 90 in Pancreatic Cancer Impairs Insulin-like Growth Factor-I Receptor Signaling, Disrupts an Interleukin-6/Signal-Transducer and Activator of Transcription 3/Hypoxia-Inducible Factor-1α Autocrine Loop, and Reduces Orthotopic Tumor Growth. Clinical Cancer Research. 2007;13:6459-68.

Lesprit P, Godeau B, Authier FJ, Soubrier M, Zuber M, Larroche C, Viard JP, Wechsler B, Gherardi R. Pulmonary hypertension in POEMS syndrome: a new feature mediated by cytokines. Am J Respir Crit Care Med 1998 Mar;157(3 Pt 1):907-11. 1998;157:907-11.

Levin ER. Endothelins. New England Journal of Medicine. 1995;333:356-63.

Lévy M, Maurey C, Celermajer DS, Vouhé PR, Danel C, Bonnet D, et al. Impaired Apoptosis of Pulmonary Endothelial Cells Is Associated With Intimal Proliferation and Irreversibility of Pulmonary Hypertension in Congenital Heart Disease. Journal of the American College of Cardiology. 2007;49:803-10.

Li J, Tian Z, Zheng H-Y, Zhang W, Duan M-H, Liu Y-T, et al. Pulmonary hypertension in POEMS syndrome. Haematologica. 2012;98:393-8.

Ma J, Zhang L, Han W, Shen T, Ma C, Liu Y, et al. Activation of JNK/c-Jun is required for the proliferation, survival, and angiogenesis induced by EET in pulmonary artery endothelial cells. Journal of Lipid Research. 2012;53:1093-105.

Markewitz BA, Kohan DE, Michael JR. Hypoxia decreases endothelin-1 synthesis by rat lung endothelial cells. Am J Physiol. 1995;269:L215-20.

Martignoni M, Groothuis GM, de Kanter R. Species differences between mouse, rat, dog, monkey and human CYP-mediated drug metabolism, inhibition and induction. Expert Opinion on Drug Metabolism & Toxicology. 2006;2:875-94.

Mautino G, Henriquet C, Gougat C, Le Cam A, Dayer JM, Bousquet J, Capony F. Increased expression of tissue inhibitor of metalloproteinase-1 and loss of correlation with matrix metalloproteinase-9 by macrophages in asthma. Lab Invest. 1999 79(1):39-47.

Miyata M, Ito M, Sasajima T, Ohira H, Kasukawa R. EFfect of a serotonin receptor antagonist on interleukin-6-induced pulmonary hypertension in rats*. CHEST Journal. 2001;119:554-61.

Mizuno S, Farkas L, Al Husseini A, Farkas D, Gomez-Arroyo J, Kraskauskas D, et al. Severe Pulmonary Arterial Hypertension Induced by SU5416 and Ovalbumin Immunization. American Journal of Respiratory Cell and Molecular Biology. 2012;47:679-87.

Naomi S, Iwaoka T, Disashi T, Inoue J, Kanesaka Y, Tokunaga H, et al. Endothelin-1 Inhibits Endothelin-Converting Enzyme-1 Expression in Cultured Rat Pulmonary Endothelial Cells. Circulation. 1998;97:234-6.

Nelson DR, Zeldin DC, Hoffman SM, Maltais LJ, Wain HM, Nebert DW. Comparison of cytochrome P450 (CYP) genes from the mouse and human genomes, including nomenclature recommendations for genes, pseudogenes and alternative-splice variants. Pharmacogenetics. 2004;14(1):1-18.

Nilsson CL, Dillon R, Devakumar A et al. Quantitative Phosphoproteomic Analysis of the STAT3/IL-6/HIF1α Signaling Network: An Initial Study in GSC11 Glioblastoma Stem Cells. J Proteome Res. 2010;9:430-43.

Nishimaki T, Aotsuka S, Kondo H, Yamamoto K, Takasaki Y, Sumiya M, Yokohari R. Immunological analysis of pulmonary hypertension in connective tissue diseases. J Rheumatol. 1999;Nov;26(11):2357-62.

Nozik-Grayck E, Suliman HB, Majka S, Albietz J, Van Rheen Z, Roush K, et al. Lung EC-SOD overexpression attenuates hypoxic induction of Egr-1 and chronic hypoxic pulmonary vascular remodeling. American Journal of Physiology-Lung Cellular and Molecular Physiology. 2008;295:L422-L30.

Perrella MA, Edell ES, Krowka MJ, Cortese DA, Burnett JC Jr. Endothelium-derived relaxing factor in pulmonary and renal circulations during hypoxia. Am J Physiol. 1992;263:R45-50.

Pietra GG, Capron F, Stewart S, Leone O, Humbert M, Robbins IM, et al. Pathologic assessment of vasculopathies in pulmonary hypertension. Journal of the American College of Cardiology. 2004;43:S25-S32.

Pinto RF, Higuchi MdeL, Aiello VD. Decreased numbers of T-lymphocytes and predominance of recently recruited macrophages in the walls of peripheral pulmonary arteries from 26 patients with pulmonary hypertension secondary to congenital cardiac shunts. Cardiovascular Pathology. 2004;13:268-75.

Price LC, Montani D, Tcherakian C, Dorfmuller P, Souza R, Gambaryan N, et al. Dexamethasone reverses monocrotaline-induced pulmonary arterial hypertension in rats. European Respiratory Journal. 2011;37:813-22.

Rodríguez-Pascual F, Redondo-Horcajo M, Lamas S. Functional Cooperation Between Smad Proteins and Activator Protein-1 Regulates Transforming Growth Factor- Beta-Mediated Induction of Endothelin-1 Expression. Circulation Research. 2003;92:1288-95.

Rodríguez-Pascual F, Reimunde FM, Redondo-Horcajo M, Lamas S. Transforming growth factor-beta induces endothelin-1 expression through activation of the Smad signaling pathway. Journal of cardiovascular pharmacology 2004;44 Suppl 1:S39-42.

Rubens C, Ewert R, Halank M, Wensel R, Orzechowski H-D, Schultheiss H-P, et al. BIg endothelin-1 and endothelin-1 plasma levels are correlated with the severity of primary pulmonary hypertension*. CHEST Journal. 2001;120:1562-9.

Sakao S, Taraseviciene-Stewart L, Lee JD, Wood K, Cool CD, Voelkel NF. Initial apoptosis is followed by increased proliferation of apoptosis-resistant endothelial cells. The FASEB Journal. 2005;19(9):1178-80.

Salameh A, Galvagni F, Bardelli M, Bussolino F, Oliviero S. Direct recruitment of CRK and GRB2 to VEGFR-3 induces proliferation, migration, and survival of endothelial cells through the activation of ERK, AKT, and JNK pathways. Blood. 2005;106:3423-31.

Sanchez O, Marcos E, Perros Fdr, Fadel E, Tu L, Humbert M, et al. Role of Endothelium-derived CC Chemokine Ligand 2 in Idiopathic Pulmonary Arterial Hypertension. American Journal of Respiratory and Critical Care Medicine. 2007;176:1041-7.

Savale L, Izikki M, Tu L, Rideau D, Raffestin B, Maitre B, et al. 085 Attenuated hypoxic pulmonary hypertension in interleukin-6 knockout mice. Revue Des Maladies Respiratoires. 2007;24:1235-.

Savale L, Tu L, Rideau D, Izziki M, Maitre B, Adnot S, et al. Impact of interleukin-6 on hypoxia-induced pulmonary hypertension and lung inflammation in mice. Respiratory Research C7 - 6. 2009;10:1-13.

Soon E, Holmes AM, Treacy CM, Doughty NJ, Southgate L, Machado RD, et al. Elevated Levels of Inflammatory Cytokines Predict Survival in Idiopathic and Familial Pulmonary Arterial Hypertension. Circulation. 2010;122:920-7.

Steiner MK, Syrkina OL, Kolliputi N, Mark EJ, Hales CA, Waxman AB. Interleukin-6 Overexpression Induces Pulmonary Hypertension. Circulation Research. 2009;104:236-44.

Stenmark KR, Fagan KA, Frid MG. Hypoxia-Induced Pulmonary Vascular Remodeling: Cellular and Molecular Mechanisms. Circulation Research. 2006;99:675-91.

Tada Y, Laudi S, Harral J, Carr M, Ivester C, Tanabe N, Takiguchi Y, Tatsumi K, Kuriyama T, Nichols WC, West J. Murine pulmonary response to chronic hypoxia is strain specific. Exp Lung Res. 2008;34(6):313-23.

Taraseviciene-Stewart L, Kasahara Y, Alger L, Hirth P et al. Inhibition of the VEGF receptor 2 combined with chronic hypoxia causes cell death-dependent pulmonary endothelial cell proliferation and severe pulmonary hypertension. The FASEB Journal. 2001;15:427-38.

Taraseviciene-Stewart L, Scerbavicius R, Choe K-H, Cool C, Wood K, Tuder RM, et al. Simvastatin causes endothelial cell apoptosis and attenuates severe pulmonary hypertension. American Journal of Physiology - Lung Cellular and Molecular Physiology. 2006;291:L668-L76.

Taylor JL, Hattle JM, Dreitz SA, Troudt JM, Izzo LS, Basaraba RJ, et al. Role for Matrix Metalloproteinase 9 in Granuloma Formation during Pulmonary Mycobacterium tuberculosis Infection. Infection and Immunity. 2006;74:6135-44.

Thenappan T, Shah SJ, Rich S, Gomberg-Maitland M. A USA-based registry for pulmonary arterial hypertension: 1982-2006. European Respiratory Journal. 2007;30:1103-10.

Tuder RM, Chacon M, Alger L, Wang J, Taraseviciene-Stewart L, Kasahara Y, et al. Expression of angiogenesis-related molecules in plexiform lesions in severe pulmonary hypertension: evidence for a process of disordered angiogenesis. The Journal of Pathology. 2001a;195:367-74.

Tuder RM, Groves B, Badesch DB, and Voelkel NF. Exuberant endothelial cell growth and elements of inflammation are present in plexiform lesions of pulmonary hypertension. Am J Pathol. 1994;144:275-85.

Tuder RM, Yeager ME, Geraci M, Golpon HA, Voelkel NF. Severe pulmonary hypertension after the discovery of the familial primary pulmonary hypertension gene. European Respiratory Journal. 2001b;17:1065-9.

Voelkel NF, Tuder RM. Hypoxia-induced pulmonary vascular remodeling: a model for what human disease? J Clin Invest. 2000;106:733-8.

Voelkel NF, Tuder RM. Cellular and Molecular Biology of Vascular Smooth Muscle Cells in Pulmonary Hypertension. Pulmonary Pharmacology & Therapeutics. 1997;10:231-41.

Yao JS, Zhai W, Young WL, Yang G-Y. Interleukin-6 triggers human cerebral endothelial cells proliferation and migration: The role for KDR and MMP-9. Biochemical and Biophysical Research Communications. 2006;342:1396-404.

Yao JS, Zhai W, Fan Y, Lawton MT, Barbaro NM, Young WL, Yang GY. "Interleukin-6 upregulates expression of KDR and stimulates proliferation of human cerebrovascular smooth muscle cells," expression of KDR and stimulates proliferation of human cerebrovascular smooth muscle cells,". Journal of Cerebral Blood Flow and Metabolism. 2007;27:510-20.

Ye C, Sweeny D, Sukbuntherng J, Zhang Q, Tan W, Wong S, et al. Distribution, metabolism, and excretion of the anti-angiogenic compound SU5416. Toxicology in Vitro. 2006;20:154-62.

Yogi A, Callera GE, Montezano ACI, Aranha AB, Tostes RC, Schiffrin EL, et al. Endothelin-1, but not Ang II, Activates MAP Kinases Through c-Src Independent Ras-Raf Dependent Pathways in Vascular Smooth Muscle Cells. Arteriosclerosis, Thrombosis, and Vascular Biology. 2007;27:1960-7.

Yoo JK, Kwon H, Khil L-Y, Zhang L, Jun H-S, Yoon J-W. IL-18 Induces Monocyte Chemotactic Protein-1 Production in Macrophages through the Phosphatidylinositol 3-Kinase/Akt and MEK/ERK1/2 Pathways. The Journal of Immunology. 2005;175:8280-6.

Yoshimura T, Robinson EA, Tanaka S, Appella E, Leonard EJ. Purification and amino acid analysis of two human monocyte chemoattractants produced by phytohemagglutinin-stimulated human blood mononuclear leukocytes. The Journal of Immunology. 1989;142:1956-62.

Yu L, Hales CA. Hypoxia Does neither Stimulate Pulmonary Artery Endothelial Cell Proliferation in Mice and Rats with Pulmonary Hypertension and Vascular Remodeling nor in Human Pulmonary Artery Endothelial Cells. Journal of Vascular Research. 2011;48:465-75.

Zhang XL, Topley N, Ito T, Phillips A. Interleukin-6 Regulation of Transforming Growth Factor (TGF)-beta Receptor Compartmentalization and Turnover Enhances TGF-beta1 Signaling. Journal of Biological Chemistry. 2005;280:12239-45.

Zhang YM, Wang KQ, Zhou GM, Zuo J, Ge JB. Endothelin-1 promoted proliferation of vascular smooth muscle cell through pathway of extracellular signal-regulated kinase and cyclin D1. Acta Pharmacol Sin. 2003;24(6):563-8.

FIGURE LEGENDS

Figure 1: **Effect of vascular endothelial growth factor receptor (VEGFR) inhibitor (SU5416) on lung vessels.** (A) Experimental setup: three-week-old male SV129 mice were injected subcutaneously three times a week with SU5416 (20mg/kg) or vehicle combined with exposure to hypoxic environment (10% O_2) for three weeks. Normoxia was used as control. (B, C) Representative immunoblot protein expression and quantification of cleaved caspase-3. Anti-GAPDH was used as a loading control. Diagrams show the densitometry quantification (n=4). (D) Right ventricular (RV) systolic pressure (RVSP) was recorded via needle directly assessed to RV lumen at subxiphoid site. (E) RV/left ventricle plus septum weight ratio (Fulton index). (F) RV (mg)/body weight (g) ratio. Data are expressed as means ± SEM for 5-6 mice per group. Statistical differences (**P*<0.01, ***P*< 0.001, ****P*< 0.0001) were determined using *t* test.

Figure 2: **SU5416 enhanced chronic hypoxia-induced vascular remodeling with development of neointimal occlusive lesions.** (A) (a-f) Representative double immunofluorescent (a-c) and immunohistochemistry (d-f) staining images of the predominantly remodeled vessel showed completely occluded arterioles with multilayer of cells expressing vWF and severe thickening of medial layer of arterioles in hypoxia combined SU5416-treated mice (c, f). No neointimal hyperplastic or occlusive lesions were noted and endothelium still remained monolayer in hypoxic and normoxic mice (a, b, d, e). Medial layer was thicker in hypoxic mice (b, e), but thinner than in hypoxia combined SU5416-treated mice (c, f).

(B) Vascular muscularization: 4-µm lung sections were stained with antibodies for α-smooth muscle actin (SMA) and von Willebrand factor (vWF). Forty pulmonary arterioles (< 100 µm) per section were blindly evaluated to the source of tissue. Based on the circumferential staining

of SMA, the vessel was determined as either non-muscularized (N), or partially muscularized (P) (<75% staining), or fully muscularized (F) (≥75% staining), then the percentage distribution of each calculated per group. Scale bars: 50 μm. Statistical differences (***P< 0.001, ****P< 0.0001) were expressed by analysis of variance.

Figure 3: **Hypoxia combined SU5416 induced endothelial cellular proliferation**. (A) Representative double immunofluorescent staining images showed concentric neointimal proliferation with increasing Proliferating Cell Nuclear Antigen (PCNA) expression in the thicken endothelial layer (expressing vWF) leading to arteriole occlusion in hypoxia combined SU5416-treated mice (c), whereas, endothelium still remained monolayer with low PCNA expression in hypoxic and normoxic mice (a, b). Scale bars: 50 μm. (B) Quantification of endothelial cells expressing PCNA/vessel. (C, D, E, G) The relative mRNA expression of VEGF-A, VEGF-R2, MMP-9 and Bcl-2 to GAPDH in lung lysates was analyzed by quantitative real-time RT-PCR (n=5-6). (F, H, I, L) Representative immunoblot protein expression of VEGF-R2, phosphorylated c-Jun N-terminal kinases (pJNK), phosphorylated extracellular-signal regulated kinases and Bcl-2 (pERK1/2) and (J, K, M) quantification of pJNK/JNK, pERK1/2/GAPDH and Bcl-2/GAPDH. Anti-GAPDH was used as a loading control, (n=4). Statistical differences (*P <0.05, **P< 0.01, ***P< 0.001) were determined using *t* test.

Figure 4: **Increase of inflammatory response in hypoxia combined SU5416-treated mice versus in hypoxic and normoxic mice.** (A) Representative immunohistochemistry staining images showed markedly increased recruitment of macrophages (Mac3 marker) in whole lung (a,b,c) and particularly in the adventitia of remodeled arterioles in hypoxia combined SU5416-

treated mice (f) versus in hypoxic (e) and normoxic (d) mice. Scale bars: 50 μm. (B) The number of macrophages in lung using the 400 x magnifications was manually counted by two independent individuals. A minimum of forty fields/lung section was counted and the result was the mean of macrophages/field. (C) The number of macrophages in adventitia was counted by two independent individuals using 400 x magnifications. A minimum of forty arterioles/lung section was counted and the result was the mean of macrophages/vessel. (D) Representative immunoblot protein expression and quantification of F4/80 in lung lysates of hypoxia combined SU5416-treated mice as well as normoxic and hypoxic mice. GAPDH was used as a loading control, (n=4). (E) Plots showed mRNA expression of MCP-1in lung lysates, normalized to GAPDH, (n=5-6). Statistical differences (*P< 0.05, **P< 0.01, ***P< 0.001) were expressed by analysis of variance.

Figure 5: **Up-regulation of interleukin-6 (IL-6) and IL-6 receptor in hypoxia combined SU5416-treated mice.** (A) Representative immunohistochemistry (a-c) and double immunofluorescent (d-i) staining images showed abundant IL-6 expression in the adventitia of remodeled arterioles in hypoxia combined SU5416-treated mice (c,f,i), whereas no detection in normoxic mice (a,d,g) and little expression in hypoxic mice (b,e,h). Scale bars: 50 μm. (B) Representative immunoblot and quantification of IL-6 expression in lung lysates of hypoxia combined SU5416-treated mice as well as hypoxic and normoxic mice. Immunoblots were representative of lungs from 4 individuals for each group. (C, D) Relative mRNA expression of IL-6 and IL-6 receptor to GADPH in lung lysates. The results were expressed as means ± SEM of 5-6 lung lysates per group. Statistical differences (*P< 0.05, **P< 0.01, ***P< 0.001) were determined using *t* test.

Figure 6: **Dysregulated expression of genes regarding transforming growth factor-β (TGF-β)/bone morphogenic protein (BMP) pathway and hypoxia inducible factor-1α (HIF-1α) signaling machinery in mice exposed to hypoxia combined with/without SU5416.** (A, B) Representative immunoblot protein expression of HIF-1α and pSmad3 and (C, D) quantification of HIF-1α and pSmad3, respectively. Immunoblots were representative of lungs from 4 individuals for each group. (E, F) Relative mRNA expression of TGF-β and BMPRII to GAPDH. The results were expressed as means ± SEM of 5-6 lung lysates per group. Statistical differences (**P*< 0.05, ***P*< 0.01, ****P*< 0.001) were determined using *t* test.

Figure 7: **Lung profiling from hypoxia combined SU5416-treated mice showed dysregulation of genes regarding endothelin signaling machinery, whereas no change in hypoxic mice**. (A, B, D) Relative mRNA expression of ET-1, ETAR and ETBR to GADPH in lung lysates of normoxic, hypoxic, and hypoxia combined SU5416-treated mice normalized to normoxia group, (n=5-6). (C) Representative protein expression of ETAR from lungs of normoxic, hypoxic and hypoxia combined SU5416-treated mice. Densitometry was performed and normalized for GAPDH, (n=4). (E) Double immunofluorescent staining with antibody anti-SMA and ETAR showed the expression of ETAR in medial layer (SMA staining) in pulmonary arterioles of hypoxia combined SU5416-treated mice, but not in that of hypoxic and normoxic ones. Scale bars: 50 μm. Statistical differences (**P* < 0.05, ***P*< 0.01) were determined using *t* test.

Figure 8: **Effects of hypoxia (1% O_2), hypoxia combined with SU5416 (15nM) on IL-6 expression in activated macrophages transformed from human monocytic cell line (THP-1)**

under phorbol myristate acetate (PMA) treatment. (A) Relative mRNA expression of IL-6 normalized to 18S, (n=4). (B) Representative immunoblot and quantification of IL-6 (n=4). GAPDH was used as a loading control, (n=4). Statistical differences (*P< 0.05, **P< 0.01) were determined using *t* test.

*Figure 9**:*** **Effect of IL-6 treatment (50ng/ml) on ET-1, ETBR expression and proliferation of MS1** (mouse pancreatic endothelial cell line) **and primary mouse pulmonary endothelial cells (pmPECs).** (A, B, D, E) Relative mRNA expression of ET-1, ETBR to GAPDH in MS1 (A, B) and pmPECs (D, E) normalized to control. (C) IL-6 stimulated MS1 proliferation measured by WST-1 assay.

Figure 1

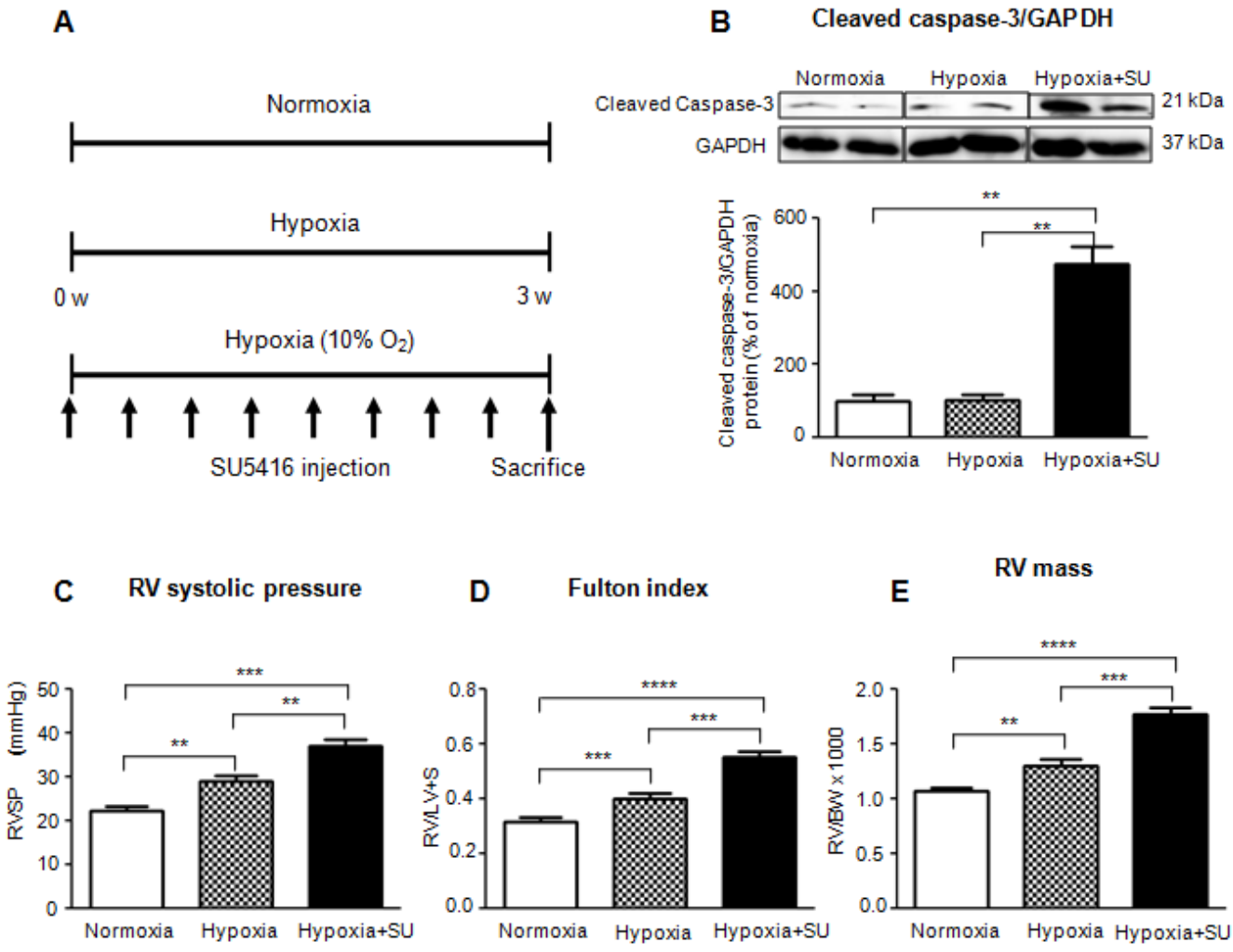
A
Normoxia
Hypoxia
0 w
3 w
Hypoxia (10% O2)
SU5416 injection
Sacrifice
B
Cleaved caspase-3/GAPDH
Normoxia
Hypoxia
Hypoxia+SU
Cleaved Caspase-3
21 kDa
GAPDH
37 kDa
Cleaved caspase-3/GAPDH protein (% of normoxia)
600
400
200
0
**
**
Normoxia
Hypoxia
Hypoxia+SU
C
RV systolic pressure
RVSP (mmHg)
50
40
30
20
10
0
***
**
**
Normoxia
Hypoxia
Hypoxia+SU
D
Fulton index
RV/LV+S
0.8
0.6
0.4
0.2
0.0
****
***
***
Normoxia
Hypoxia
Hypoxia+SU
E
RV mass
RV/BW x 1000
2.0
1.5
1.0
0.5
0.0
****
***
**
Normoxia
Hypoxia
Hypoxia+SU

Figure 2

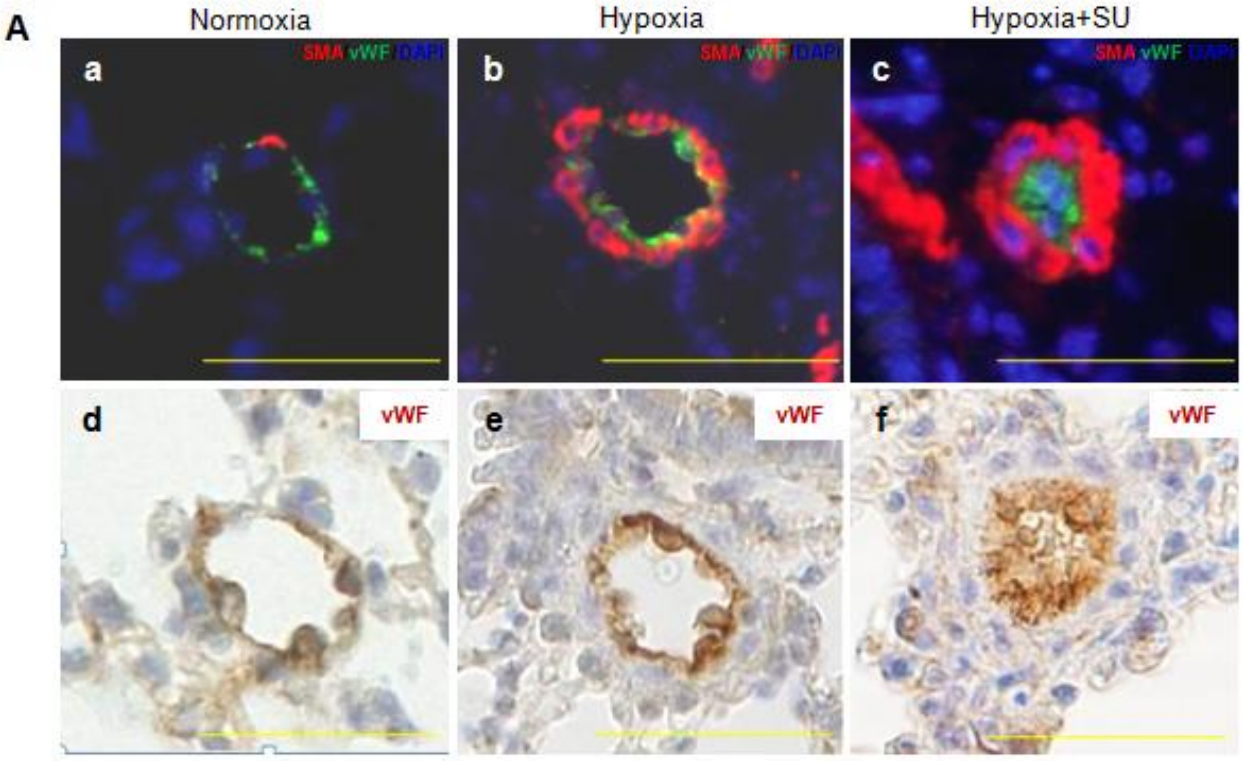
A
Normoxia
Hypoxia
Hypoxia+SU
a
b
c
SMA vWF DAPI
d
e
f
vWF

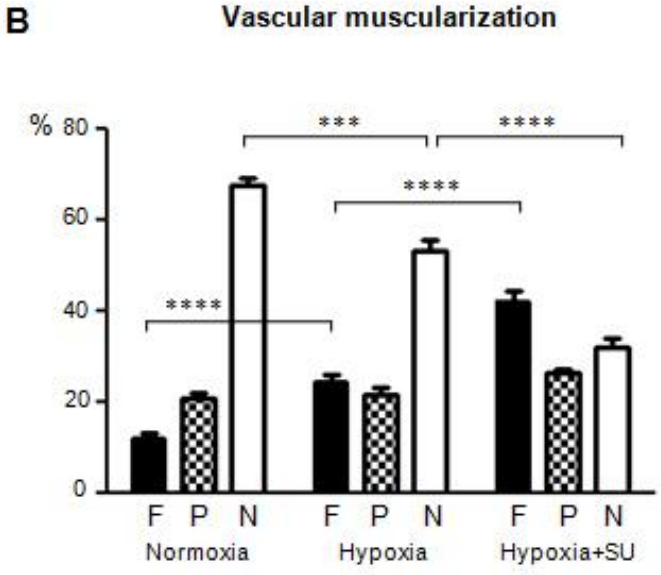
B
Vascular muscularization
%
80
60
40
20
0
***
****
****
****
F P N F P N F P N
Normoxia
Hypoxia
Hypoxia+SU

Figure 3

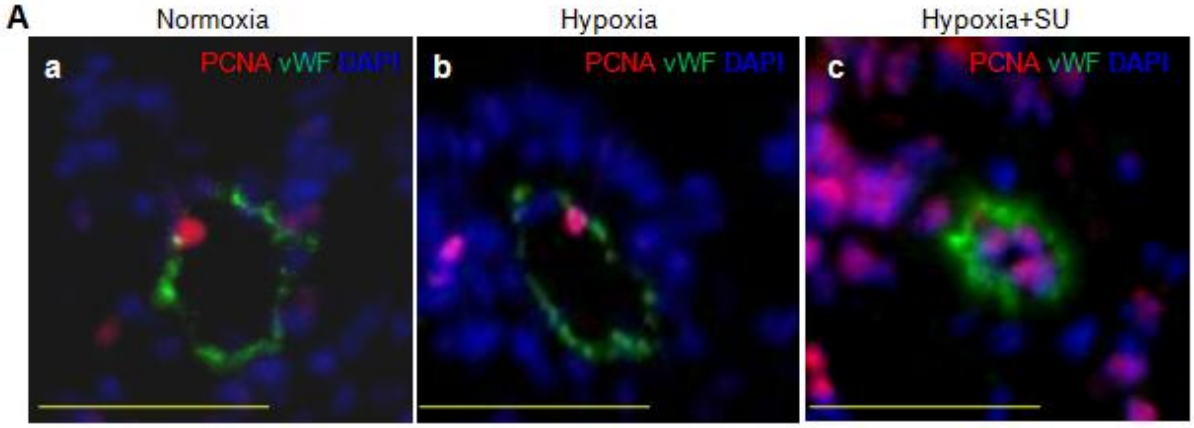
A
Normoxia
Hypoxia
Hypoxia+SU
a
PCNA vWF DAPI
b
PCNA vWF DAPI
c
PCNA vWF DAPI

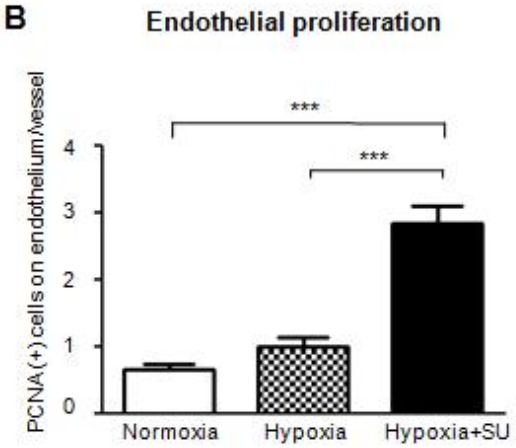
B
Endothelial proliferation
PCNA(+) cells on endothelium/vessel
***
***
0
1
2
3
4
Normoxia
Hypoxia
Hypoxia+SU

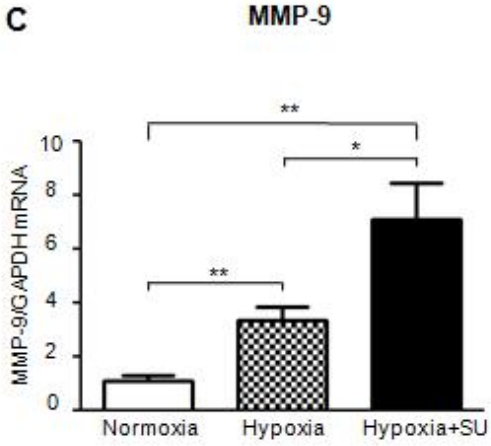
C
MMP-9
MMP-9/GAPDH mRNA
**
*
**
0
2
4
6
8
10
Normoxia
Hypoxia
Hypoxia+SU

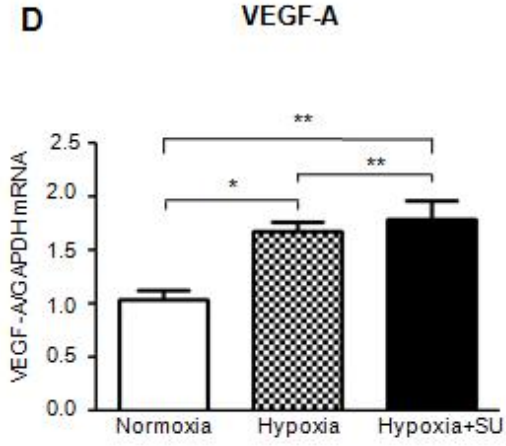
D
VEGF-A
VEGF-A/GAPDH mRNA
**
*
**
0.0
0.5
1.0
1.5
2.0
2.5
Normoxia
Hypoxia
Hypoxia+SU

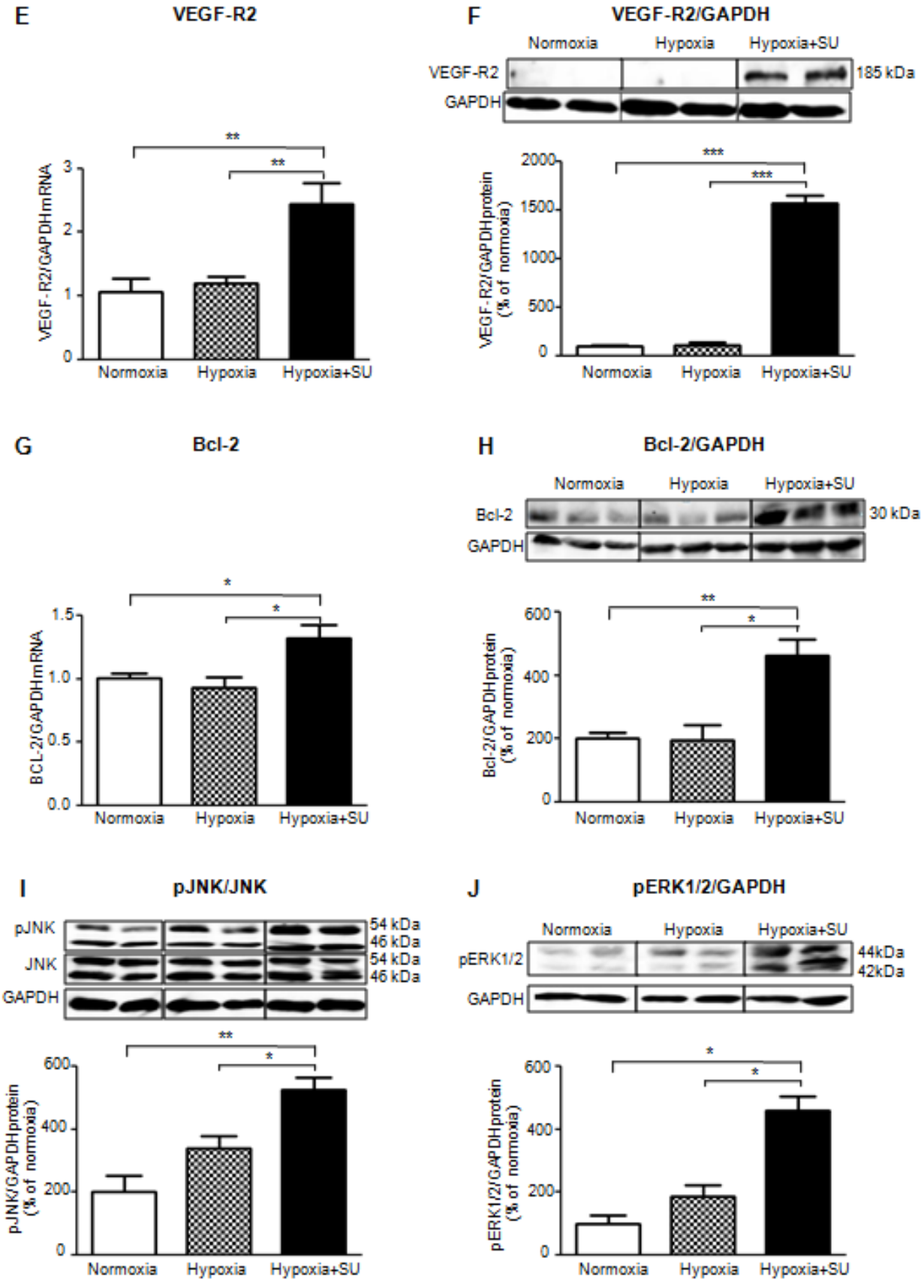
E
VEGF-R2
VEGF-R2/GAPDHmRNA
Normoxia
Hypoxia
Hypoxia+SU
F
VEGF-R2/GAPDH
Normoxia
Hypoxia
Hypoxia+SU
VEGF-R2
GAPDH
185 kDa
VEGF-R2/GAPDHprotein (% of normoxia)
G
Bcl-2
BCL-2/GAPDHmRNA
H
Bcl-2/GAPDH
Bcl-2
GAPDH
30 kDa
Bcl-2/GAPDHprotein (% of normoxia)
I
pJNK/JNK
pJNK
JNK
GAPDH
54 kDa
46 kDa
54 kDa
46 kDa
pJNK/GAPDHprotein (% of normoxia)
J
pERK1/2/GAPDH
pERK1/2
GAPDH
44kDa
42kDa
pERK1/2/GAPDHprotein (% of normoxia)

Figure 4

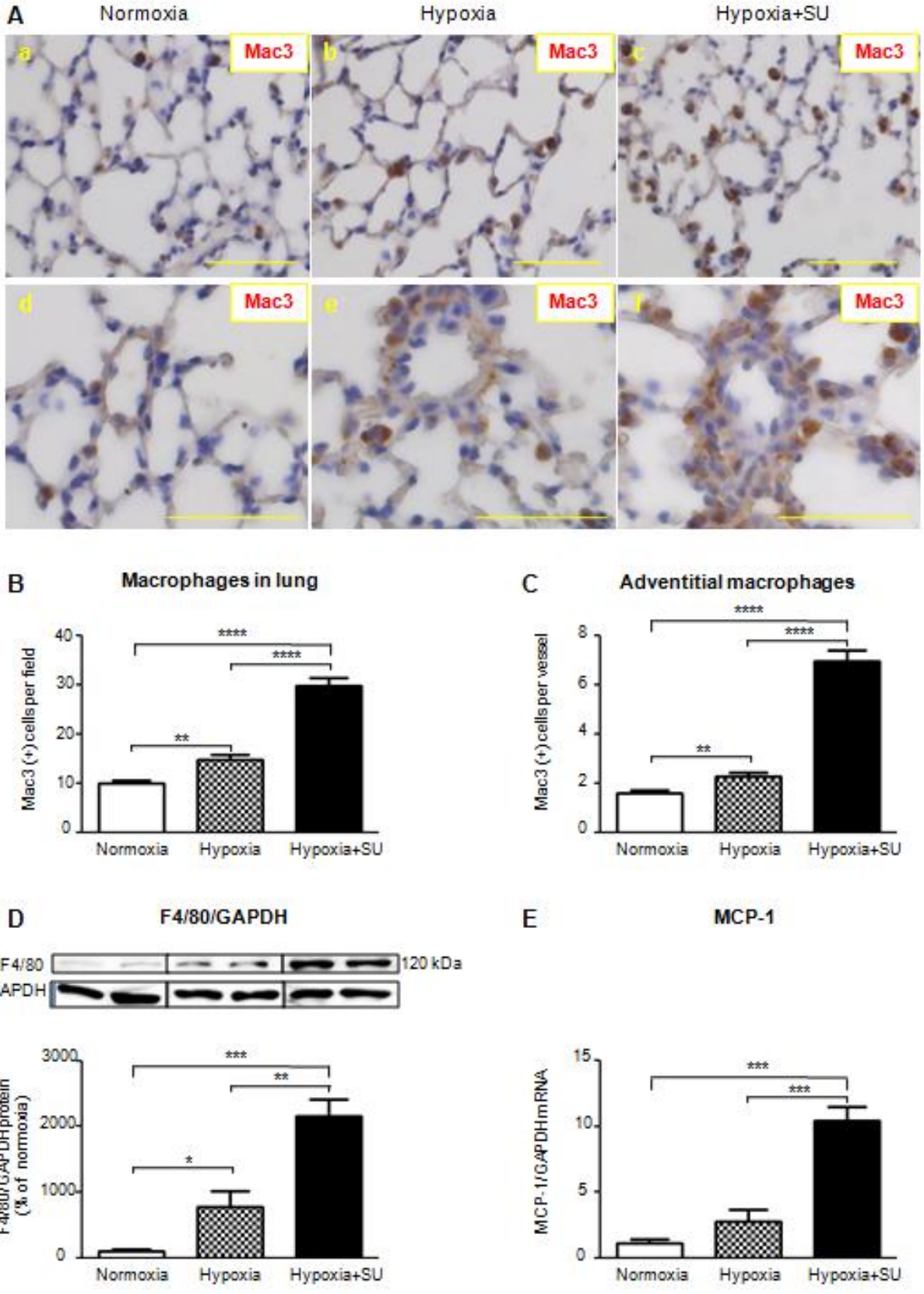
A
Normoxia
Hypoxia
Hypoxia+SU
Mac3
B
Macrophages in lung
Mac3 (+) cells per field
Normoxia
Hypoxia
Hypoxia+SU
C
Adventitial macrophages
Mac3 (+) cells per vessel
D
F4/80/GAPDH
F4/80
GAPDH
120 kDa
F4/80/GAPDH protein (% of normoxia)
E
MCP-1
MCP-1/GAPDH mRNA

Figure 5

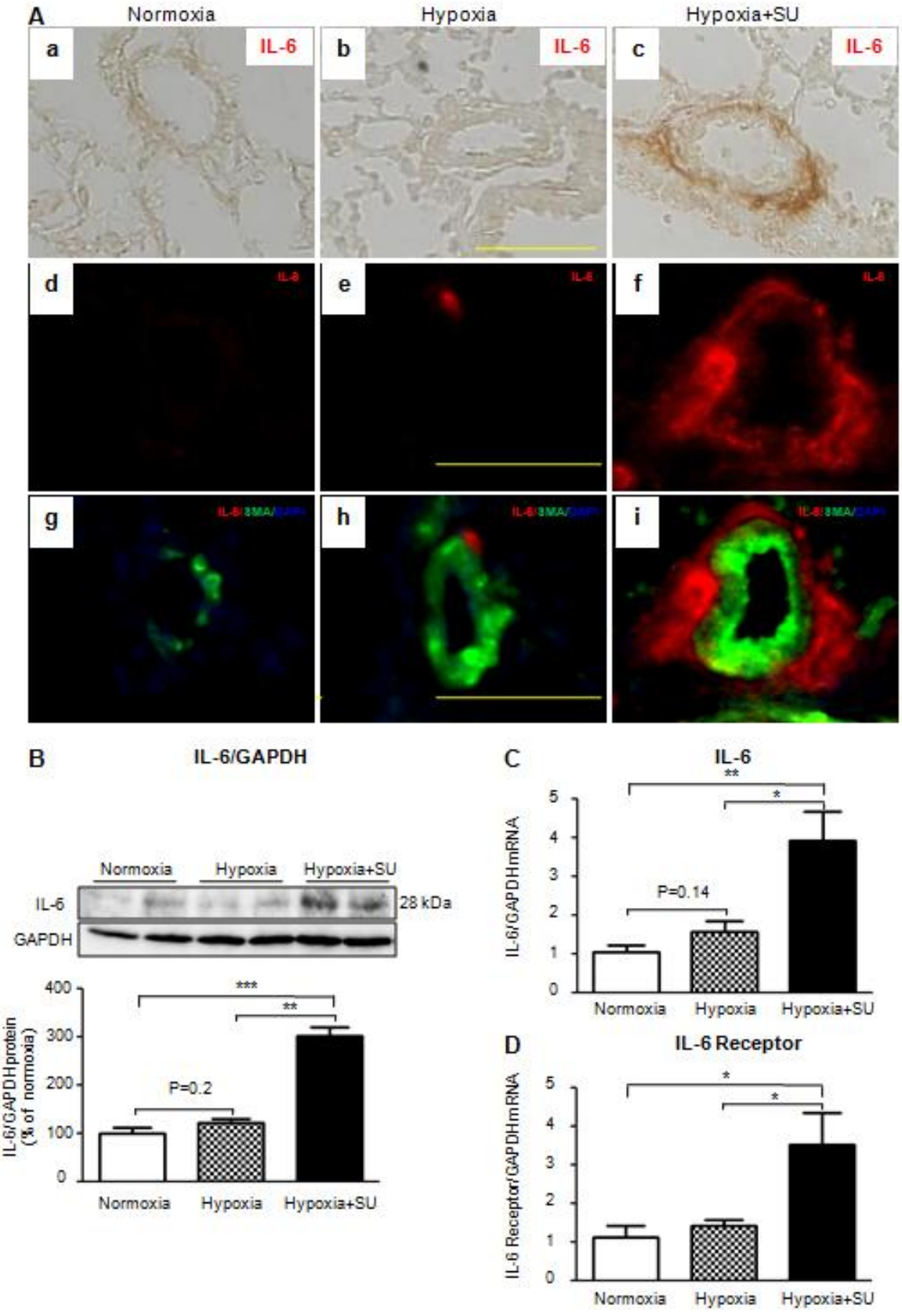
A
Normoxia
Hypoxia
Hypoxia+SU
a
b
c
IL-6
d
e
f
g
h
i
B
IL-6/GAPDH
Normoxia
Hypoxia
Hypoxia+SU
IL-6
GAPDH
28 kDa
IL-6/GAPDHprotein (% of normoxia)
400
300
200
100
0
***
**
P=0.2
C
IL-6
IL-6/GAPDHmRNA
5
4
3
2
1
0
**
*
P=0.14
D
IL-6 Receptor
IL-6 Receptor/GAPDHmRNA

Figure 6

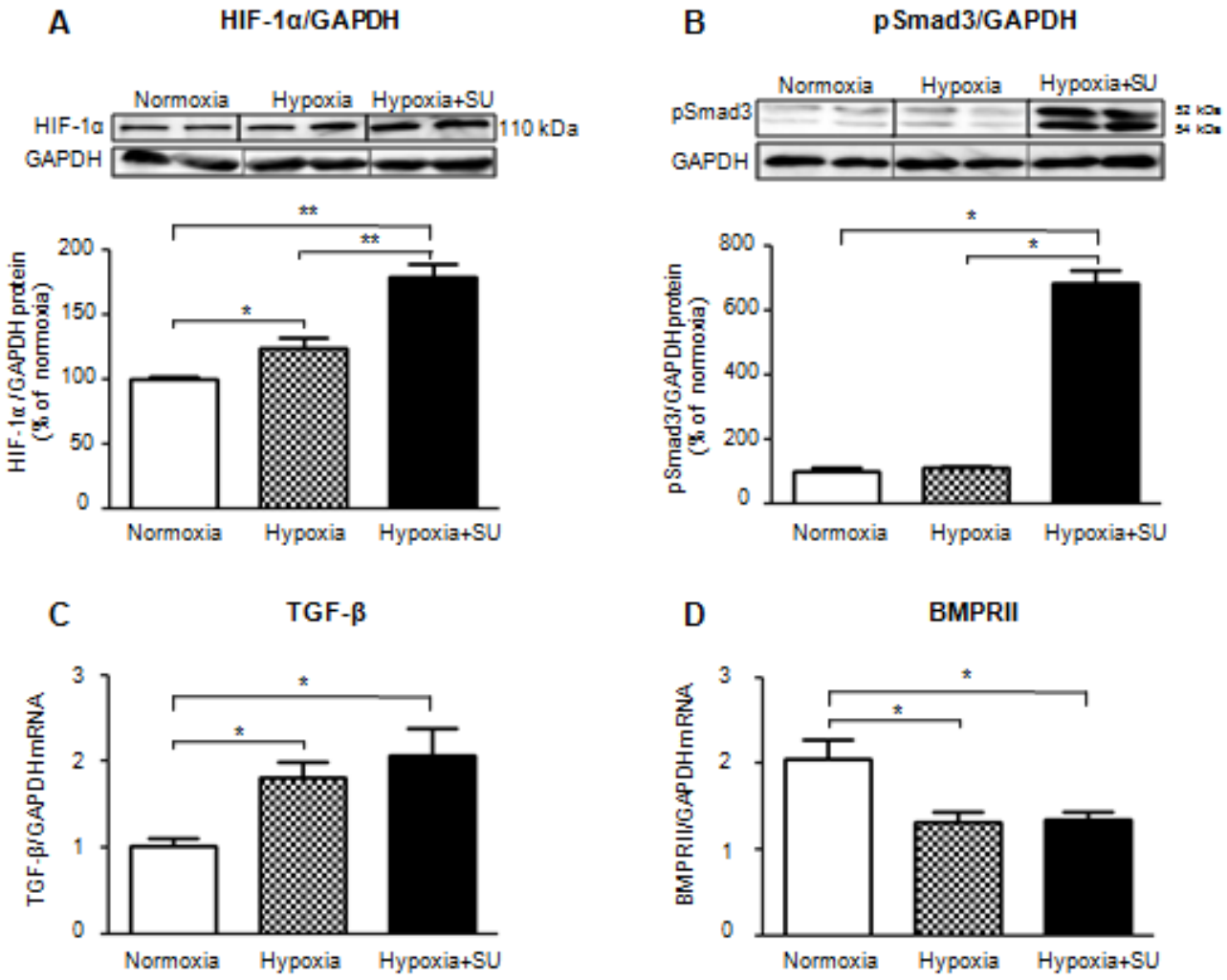
A
HIF-1α/GAPDH
Normoxia
Hypoxia
Hypoxia+SU
HIF-1α
GAPDH
110 kDa
HIF-1α /GAPDH protein (% of normoxia)
200
150
100
50
0
**
**
*
Normoxia
Hypoxia
Hypoxia+SU
B
pSmad3/GAPDH
Normoxia
Hypoxia
Hypoxia+SU
pSmad3
GAPDH
52 kDa
54 kDa
pSmad3/GAPDH protein (% of normoxia)
800
600
400
200
0
*
*
Normoxia
Hypoxia
Hypoxia+SU
C
TGF-β
TGF-β/GAPDH mRNA
3
2
1
0
*
*
Normoxia
Hypoxia
Hypoxia+SU
D
BMPRII
BMPRII/GAPDH mRNA
3
2
1
0
*
*
Normoxia
Hypoxia
Hypoxia+SU

Figure 7

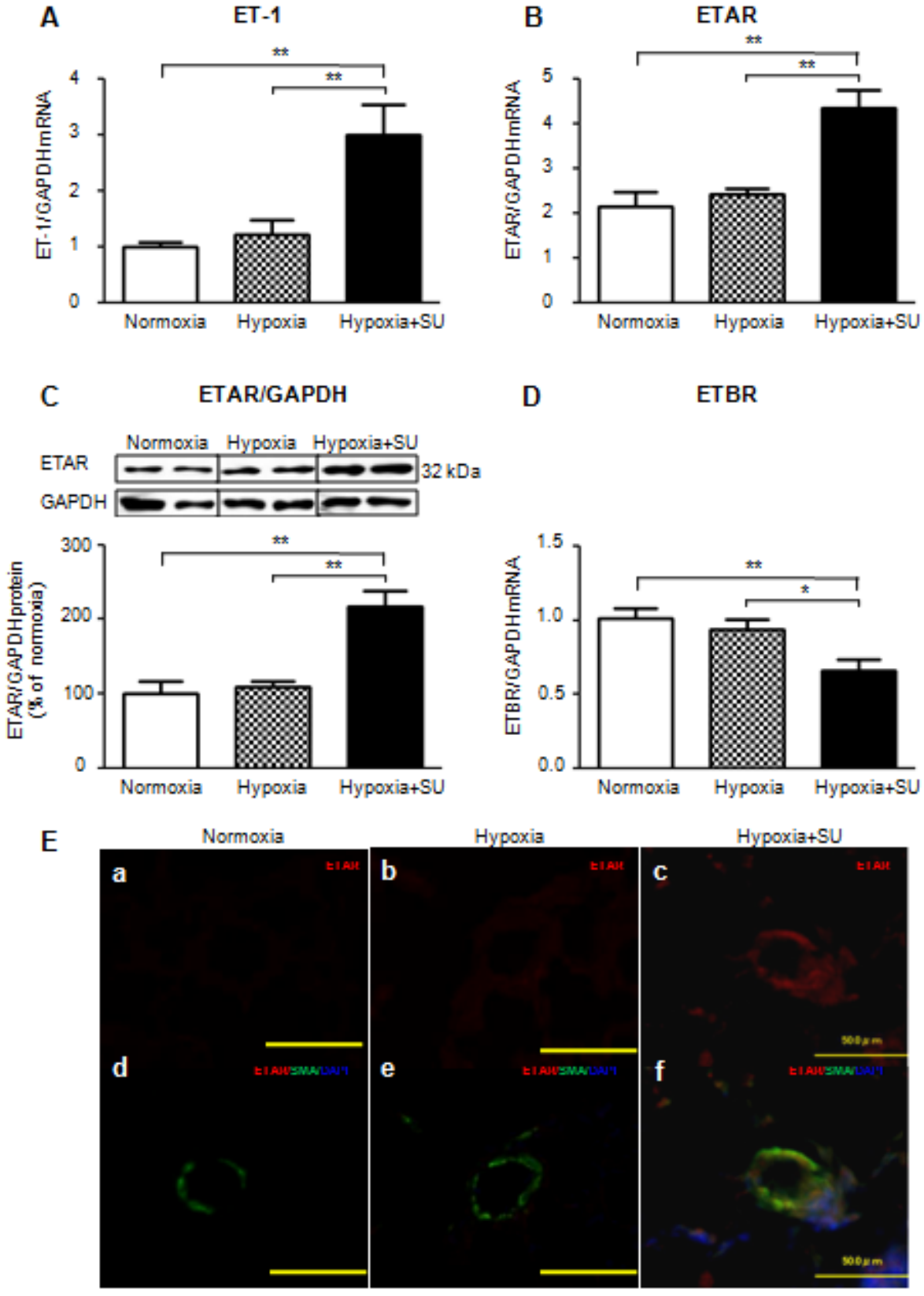
A
ET-1
ET-1/GAPDHmRNA
Normoxia
Hypoxia
Hypoxia+SU
B
ETAR
ETAR/GAPDHmRNA
C
ETAR/GAPDH
ETAR
GAPDH
32 kDa
ETAR/GAPDHprotein (% of normoxia)
D
ETBR
ETBR/GAPDHmRNA
E
a
b
c
d
e
f

Figure 8

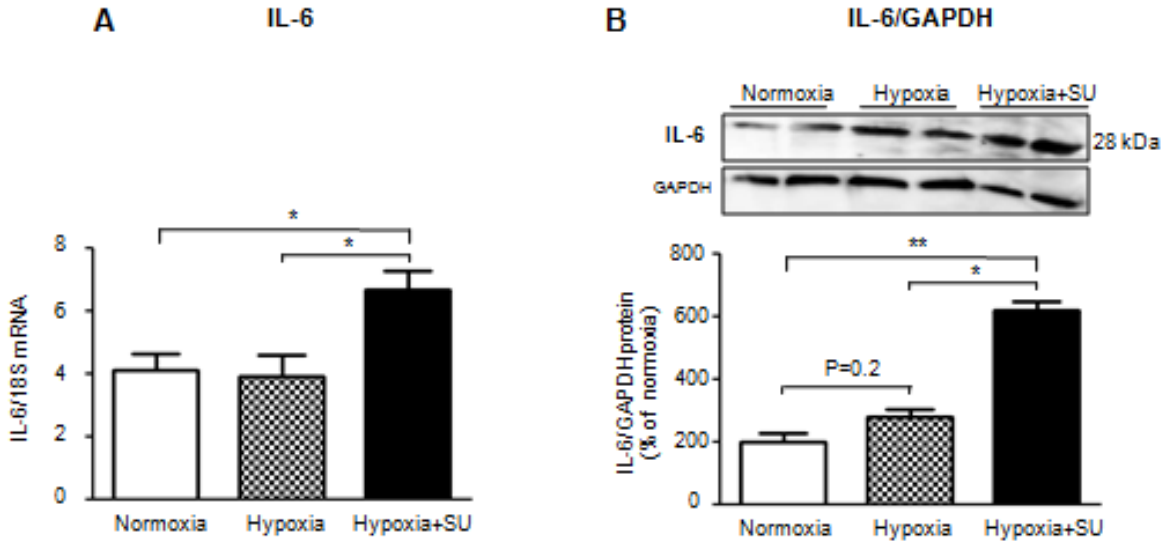

Figure 9

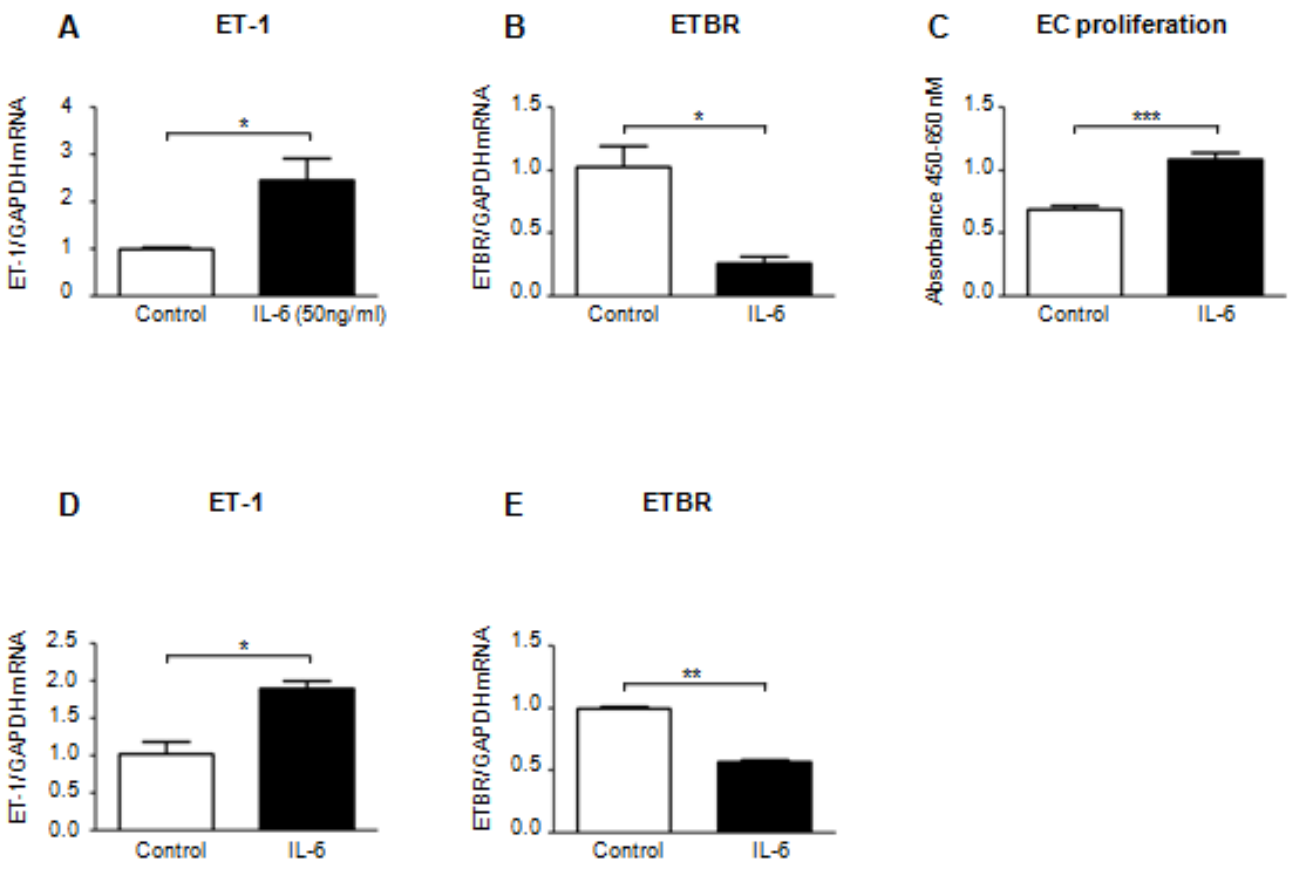

Table 1: List of primers

Gene	Forward primers (5'-3')	Reverse primers (5'-3')
mMCP1	GCATCCACGTGTTGGCTCA	CTCCAGCCTACTCATTGGGATCA
mGAPDH	TGTGTCCGTCGTGGATCTGA	TTGCTGTTGAAGTCGCAGGAG
mBMPRII	GAGCCCTCCCTTGACCTG	GTATCGACCCCGTCCAATC
mIL-6	GCTACCAAACTGGATATAATCAGGA	CCAGGTAGCTATGGTACTCCAGAA
mIL-6R	ATCCTCTGGAACCCCACAC	GAACTTTCGTACTGATCCTCGTG
mMMP-9	GCCTGGCACATAGTAGGCCC	CTTCCTAGCCAGCCGGCATC
mETBR	CATGCGCAATGGTCCCAATA	GCTCCAAATGGCCAGTCCTC
mETAR	GCTGGTTCCCTCTTCACTTAAGC	TCATGGTTGCCAGGTTAATGC
mET-1	GCCACAGACCAGGCAGTTAGA	CACCAGCTGCTGATAGATACACTTC
mBcl-2	GTGTTCCATGCACCAAGTCCA	AGGTACAGGCATTGCCGCATA
mVEGF-A	CAGTTCGAGGAAAGGGAAAGG	CACGTCTGCGGATCTTGGAC
mVEGF-R2	CCTACCTCACCTGTTTCCTGTATG	ACCATCCCACTGTCTGTCTGG
mTGF-β	TTCCGCTGCTACTGCAAGTCA	GGGTAGCGATCGAGTGTCCA
h18S	GTAACCCGTTGAACCCCATTTTCGGT	CCATCCAATCGGTAGTAGCG
hIL-6	CCAGTTGCCTTCTC	GAGGTGAGTGGCTGTCTGTG

Table 2: Baseline body weight, final body weight, and heart rate after injection of SU5416 or vehicle and exposure for 3 weeks to 10% O_2 (hypoxia) or room air (normoxia)

	Normoxia	**Hypoxia**	**Hypoxia+SU**
	n= 6	***n=6***	***n=5***
Baseline body weight (g)	9.58 ± 0.37	9.72 ± 0.27	9.92 ± 0.21
Final body weight (g)	19.90 ± 0.72	18.80 ± 0.57	17.23 ± 0.49 A,B
Heart rate (bmp)	370 ± 15	383 ± 20	392 ± 23

All values are the mean ± SEM. A: $P< 0.01$ versus normoxia and B: $P< 0.05$ versus hypoxia.
Heart rate: measured while recording right ventricular systolic pressure (RVSP)